Few-body models applied to nuclear reactions

J. A. Tostevin and J. S. Al-Khalili

Department of Physics,
School of Electronics and Physical Sciences,
University of Surrey,
Guildford GU2 7XH, United Kingdom

Abstract

In these lectures we discuss theoretical techniques for obtaining approximate descriptions of the scattering and reactions of composite nuclei over a wide range of incident energies. The approaches used calculate approximate solutions of the time-independent few-body Schrödinger equation containing two-body effective interactions between the particles. Such solutions are particularly important in direct nuclear reactions applications. We focus on projectile (or target) nuclei with structures which, to a good approximation, can be described as strongly correlated n-body systems. These n bodies can be individual nucleons or more massive clusters of many nucleons but are usually very much fewer than the number of nucleons m_p in the projectile. The deuteron and the three-nucleon systems ^{3}H and ^{3}He are exceptions for which the methods discussed are also applicable. Loosely-bound neutron- and proton-rich nuclei and highly clustered light nuclei such as ^{6}Li and ^{7}Li are usefully described as effective few-body systems and, when interacting with strong or electromagnetic probes, require the techniques presented here to account for their elastic scattering, inelastic excitation and breakup. Particular applications are provided as references.

I. INTRODUCTION

These notes deal exclusively with non-perturbative approaches. Methods such as the distorted waves Born approximation (DWBA), which treat the reactions as a first-order transition between mean field states, and their multi-step generalisations, are discussed comprehensively elsewhere [1, 2]. Similarly, perturbative semi-classical trajectory methods, inspired by Coulomb excitation theory, have been the subject of definitive texts [3] and reviews [4, 5]. We will also not discuss explicit time-dependent non-perturbative methods as there have been very few practical applications for non-nucleonic few-body nuclear systems [6].

In Sections IV through VII we discuss fully quantum mechanical approaches based on coupled channels and adiabatic approximations. Sections VIII through XII discuss eikonal, and more general impact parameter based theoretical approaches, applicable to few-body systems.

II. FEW-BODY MODEL SPACE

We consider the scattering of a n-body projectile nucleus p with incident laboratory energy E_{lab} by a structureless target t of mass m_t and charge Z_t. The projectile ground state is assumed to be a bound state $\phi_0^{(n)}$ of the n constituents with individual masses m_j and charges Z_j. Each constituent j will be assumed to interact with the target through a two-body effective interaction V_{jt} which in general is complex. In applications, the V_{jt} are usually identified with the energy-dependent phenomenological optical potentials obtained by fitting reaction data for each jt binary sub-system at the same incident energy per nucleon. Alternatively, they are calculated from theoretical multiple scattering or folding models. These effective interactions will be assumed central throughout.

In many cases, such as the deuteron, ^{6}Li and the neutron rich light nuclei ^{6}He, ^{11}Li, and ^{19}C, the projectile has only one particle stable bound state. The tidal forces on the projectile constituents will therefore couple the projectile strongly to the continuum. A major motivation for the few-body models discussed here is the realistic treatment of, and insight into the importance of, these breakup effects on scattering and direct reaction measurements and their interpretation. The coupling between these continuum excited states is also extremely important [7] and their inclusion is an important feature of all the approaches presented.

We adopt the system of coordinates shown in Figure 1 where the set of vectors $\{\vec{r}_i\}$ refer to the $n-1$ independent internal spatial coordinates of the projectile. These will be clarified in individual applications. Vectors $\{\vec{x}_j\}$ refer to the n projectile centre of mass (cm) to constituent separations, $\vec{R}$ is the target-projectile cm separation and the $\vec{R}_j = \vec{R} + \vec{x}_j$ are the j constituent coordinates relative to the target. The coordinate z–axis will be chosen along the incident beam direction $\vec{K}_0$.

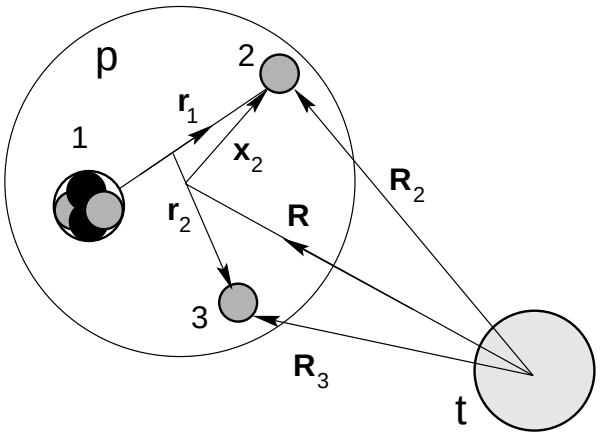

FIG.1 Definition of the coordinate vectors used in the case of a three-body projectile.

The Schrödinger equation satisfied by the scattering wave function of our effective $n+1$-body (projectile and target) system, $\Psi^{(+)}$, when the projectile is incident with wave vector $\vec{K}_0$ in the cm frame, is

$$[\,\mathcal{H} \,-\, E]\,\Psi^{(+)}_{\vec{K}_0}(\{\vec{r}_i\},\vec{R}) = 0 \quad , \tag{1}$$

with total Hamiltonian $\mathcal{H} = T_R + U(\{\vec{R}_j\}) + H_p$. Here H_p is the internal Hamiltonian for the projectile and T_R is the projectile cm kinetic energy operator. $U(\{\vec{R}_j\}) = \sum_{j=1}^{n} V_{jt}(R_j)$ is the total interaction between the projectile and the target. The n-body projectile ground state wavefunction $\phi_0^{(n)}$ satisfies

$$H_p\,\phi_0^{(n)}(\{\vec{r}_i\}) = -\varepsilon_0\,\phi_0^{(n)}(\{\vec{r}_i\})\ . \tag{2}$$

H_p will also generate an excited continuum spectrum and may support a finite number of bound or resonant excited states. We seek solutions of the few-body scattering wave function $\Psi^{(+)}_{\vec{K}_0}$ which satisfy the scattering boundary conditions

$$\Psi^{(+)}_{\vec{K}_0}(\{\vec{r}_i\},\vec{R}) = e^{i\vec{K}_0\cdot\vec{R}}\,\phi_0^{(n)}(\{\vec{r}_i\}) \,+\, \text{outgoing waves} \quad . \tag{3}$$

For a projectile with a single bound state, the outgoing waves include only elastic scattering and elastic break-up channels. More generally, the outgoing waves will also include terms from any inelastically excited bound states. The incident plane wave boundary condition stated in Eq.(3) is of course strictly correct only in the presence of screened Coulomb interactions. All formulae we use can be justified, as is usual, by considering the limit of the appropriately screened Coulomb problem.

It is implicit in the following that the methods we discuss yield only approximate solutions of the physical n-body problem. In particular one- and multi-constituent rearrangement channels are absent in the asymptotic ($R \to \infty$) regions of the derived solutions, due to our use of complex constituent-target interactions and radial and orbital angular momentum truncations [8]. In fact, all the theoretical schemes calculate approximations to $\Psi^{(+)}$ which are expected to be accurate representations of the n-body dynamics only within a restricted volume of the configuration space, or within an interaction region. Reaction or scattering

amplitudes can nevertheless be calculated accurately by using the wavefunction within an appropriate transition matrix element. We pay particular attention to the way in which the different models can be used to calculate elastic and inelastic scattering and breakup observables. We will not discuss transfer or charge-exchange reactions significantly but it is understood that, in these cases also, $\Psi^{(+)}$ should be used in the appropriate transition matrix elements [7, 8].

III. FOLDING MODEL

The folding model potential [9] between the projectile and target is the ground state expectation value of the summed constituent interactions with the target,

$$V_{00}(\vec{R}) = \langle \phi_0^{(n)} | U(\{\vec{R}_j\}) | \phi_0^{(n)} \rangle. \tag{4}$$

It provides the no-channel coupling limit of all the models we will discuss and is therefore often used as a reference from which to assess the importance of explicit breakup channel coupling and, in the case of elastic scattering, the dynamic polarisation effects introduced by such channels. Calculation of V_{00} is non-trivial for $n{>}2$ but can be carried out using numerical quadratures for $n = 3$ or Monte-Carlo sampling for larger n.

IV. CONTINUUM DISCRETISATION

The now established technique in this category is the coupled discretised continuum channels (CDCC) approach which has been formulated and applied extensively to the scattering of $n{=}2$ projectiles, such as the deuteron (n+p), ^{6}Li (α+d) and ^{7}Li (α+t) nuclei. The development of the approach and its relationship to Faddeev and other methods have been comprehensively reviewed [7, 8]. The method will not however be extended readily to systems with $n{>}2$.

By construction of a square integrable basis set $\hat{\phi}_\alpha(\vec{r})$ of relative motion states in the two-body separation $\vec{r} = \vec{R}_1 - \vec{R}_2$, on which to expand $\Psi^{(+)}(\vec{r}, \vec{R})$, the CDCC approximates the three-body Schrödinger equation as an effective two-body coupled channels equation set. The CDCC therefore works with the model space Hamiltonian

$$\mathcal{H}^{CD} = \mathcal{P}\mathcal{H}\mathcal{P}, \qquad \mathcal{P} = \sum_{\alpha=0}^{\alpha_{max}} |\hat{\phi}_\alpha\rangle\langle\hat{\phi}_\alpha|. \tag{5}$$

In outlining the technique we neglect, for simplicity, the constituent and target intrinsic spins and also target excitation. The projectile ground (excited) state total angular momentum $J_p(J_p^*)$ is then just the relative orbital angular momentum of the two constituents $\ell_0(\ell)$. We assume also that p has a single bound state. The physical spectrum of H_p is represented schematically in part (a) of Figure 2, the continuum states $\phi_{\vec{k}}(\vec{r})$ extending over relative momenta k and relative energy ε_k. The breakup channels become closed asymptotically for

$$\varepsilon_k = \hbar^2 k^2/2\mu > \hbar^2 K_0^2/2\mu_p - \varepsilon_0 \tag{6}$$

where μ and μ_p are the projectile internal and cm reduced masses.

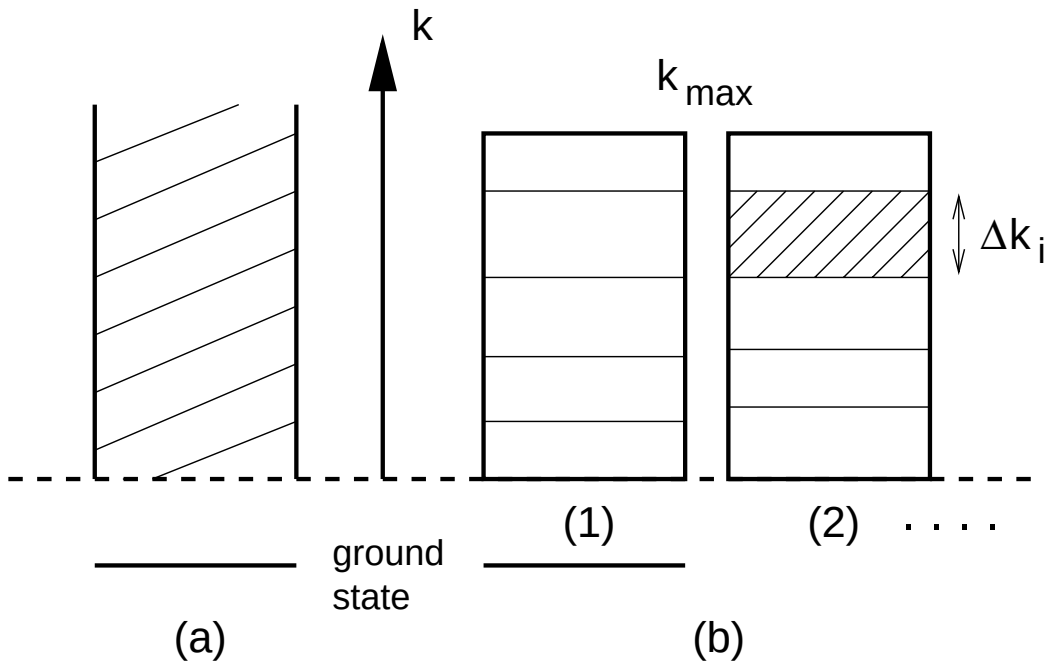

FIG.2 Schematic representation of (a) the physical spectrum of projectile states, and (b) the discretised continuum (CDCC) treatment of the continuum for different spin-parity excitations.

A. Bin state construction

The CDCC treatment of the projectile internal excitations is shown schematically in part (b) of Figure 2. Here we denote by (1), (2) $\cdots$, a physically significant set of spin-parity relative motion excitations, e.g. $J_p^* = 0, 1, 2$ in the case of a deuteron, which has $J_p = \ell_0 = 0$. For each of these J_p^* excitations the k continuum is divided (or *binned*) into a set of intervals of width $\Delta k_i = [k_i - k_{i-1}]$. The set of included J_p^* states, the number of bins $n(J_p^*)$ per spin-parity state, and their upper limit k_{max} must necessarily be truncated in practical calculations. Convergence of the calculations must then be tested for different sizes of this model space. The number of bins, their boundaries k_i, widths Δk_i and k_{max} can of course all depend on J_p^*. These parameters must be chosen to map any specific or resonant features in the continuum. For low incident energies, k_{max} may need to be chosen to include asymptotically closed channels.

For each such bin, a representative normalised square integrable relative motion wavefunction

$$\hat{\phi}^m_{i\ell}(\vec{r}) = [u^i_\ell(r)/r]\, Y^m_\ell(\hat{r}) \quad , \tag{7}$$

can be constructed. Its radial function is a superposition of the scattering states $\phi_\ell(k)$ within the bin with a weight function $f_i(k)$, i.e.

$$u^i_\ell(r) \;=\; \sqrt{\frac{2}{\pi N_i}} \int_{k_{i-1}}^{k_i} f_i(k) \phi_\ell(k,r)\, dk \;,$$

$$N_i \;=\; \int_{k_{i-1}}^{k_i} [f_i(k)]^2 dk \;. \tag{8}$$

For a non-resonant continuum, typically $f_i(k) = 1$, in which case $N_i = \Delta k_i$. The choice $f_i(k) = k$ is also useful in $\ell = 0$ continuum states and provides a more stable description of the s-wave threshold ($k \approx 0$) behavior. When treating isolated resonances [10], the choices $f_i(k) = |i\Gamma/[2(\varepsilon_k - \hat{\varepsilon}_i) + i\Gamma]|$, or $f_i(k) = \sin\delta_\ell(k)$, provide a more accurate description of the resonance strength within a bin. We have chosen the ϕ_ℓ to have normalisation

$$\phi_\ell(k,r) \to [\cos\delta_\ell(k) F_\ell(kr) + \sin\delta_\ell(k) G_\ell(kr)] \quad , \tag{9}$$

at large r, where F_ℓ and G_ℓ are the regular and irregular Coulomb functions and $\delta_\ell(k)$ is the nuclear phase shift.

The $\hat{\phi}^m_{iJ^*_p} \equiv \hat{\phi}^m_\alpha$, where $\alpha \equiv (i, J^*_p)$, thus play the role of discrete excited states and are assigned energies $\hat{\varepsilon}_\alpha = \langle\hat{\phi}_\alpha|H_p|\hat{\phi}_\alpha\rangle$. The associated asymptotic wavenumbers K_α of the cm motion of the projectile in these excited configurations are such that

$$\hbar^2 K^2_\alpha/2\mu_p + \hat{\varepsilon}_\alpha = \hbar^2 K^2_0/2\mu_p - \varepsilon_0 = E \;. \tag{10}$$

B. Coupled equations solution

These bin states, together with the ground state, constitute a conventional $\mathcal{N}+1$ state ($\mathcal{N}$=$\sum n(J^*_p)$) coupled-channels problem for solution of the CDCC approximation to $\Psi^{(+)}$

$$\begin{aligned}\Psi^{CD}_{\vec{K}_0}(\vec{r},\vec{R}) \;&=\; \phi_0(\vec{r})\hat{\chi}_0(\vec{R}) + \sum_{J^*_p,i} \hat{\phi}_{iJ^*_p}(\vec{r})\hat{\chi}_{iJ^*_p}(\vec{R}) \;, \\ &=\; \sum_{\alpha=0}^{\mathcal{N}} \hat{\phi}_\alpha(\vec{r})\hat{\chi}_\alpha(\vec{R}),\end{aligned} \tag{11}$$

where $\alpha = 0$ ($\hat{\varepsilon}_0 = -\varepsilon_0$) refers to the projectile ground state. Explicitly

$$\left[T_R \;+\; V_{\alpha\alpha}(\vec{R}) \;-\; E_\alpha\right]\hat{\chi}_\alpha(\vec{R}) = -\sum_{\beta\neq\alpha} V_{\alpha\beta}(\vec{R})\hat{\chi}_\beta(\vec{R}), \tag{12}$$

with $E_\alpha = E - \hat{\varepsilon}_\alpha$. The coupling interactions are

$$V_{\alpha\beta}(\vec{R}) = \langle\hat{\phi}_\alpha|U(\{\vec{R}_j\})|\hat{\phi}_\beta\rangle. \tag{13}$$

The evaluation of these couplings involves additional practical truncations of the CDCC model space, namely of (i) the maximum order used in the multipole expansion of the interactions U, and (ii) the maximum radius r_{bin} used in evaluating these matrix elements. These must be chosen to be consistent with the included J^*_p channels and the bin widths Δk_i and interaction ranges, respectively.

Solution of these coupled equations is carried out by usual partial wave decomposition. We expand the scattering wavefunction, for incident spin projection m, in total angular momentum eigenstates

$$\Psi^{CD}_{\vec{K}_0 m}(\vec{r},\vec{R}) = \sum_{\alpha J M_J L} C^{JM_J}_{Lm}(\vec{K}_0)\Psi^{CD}_{\alpha J M_J}(\vec{r},\vec{R}) \tag{14}$$

where we define

$$\Psi^{CD}_{\alpha J M_J}(\vec{r},\vec{R}) = \sum_{L'M'J_\alpha M_\alpha} (L'M'J_\alpha M_\alpha|JM_J) i^{L'} Y^{M'}_{L'}(\hat{R}) \times \hat{\phi}^{M_\alpha}_{J_\alpha}(\vec{r}) \, [\hat{\chi}^J_\alpha(R)/R]. \quad (15)$$

The radial coupled equations for the $\hat{\chi}$ are solved subject to the asymptotic boundary conditions

$$\hat{\chi}^J_\alpha \to F_{L'}(K_\alpha R)\delta_{0\alpha} + \widehat{\mathcal{T}}^J_{0:\alpha} H^+_{L'}(K_\alpha R), \quad (16)$$

where $H^+_L = G_L + iF_L$ is the outgoing waves Coulomb function. $\widehat{\mathcal{T}}_{0:\alpha} \equiv \widehat{\mathcal{T}}_{LJ_p:L'J^*_p}(K_\alpha)$ is the partial wave T-matrix element for exciting bin α. The coefficients C are obtained by matching the entrance channel boundary condition, and are

$$C^{JM_J}_{Lm}(\vec{K}_0) = \frac{4\pi}{K_0} \sum_M e^{i\omega_L(0)} (LMJ_p m|JM_J) Y^M_L(\widehat{K}_0)^*, \quad (17)$$

where $\omega_L(0)$ is the elastic channel Coulomb phase $\omega_L = \sigma_L - \sigma_0$. Combining results, the (partial wave summed) amplitude for excitation of excited configuration α, in angular momentum sub-state m' is

$$\widehat{\mathcal{F}}_{m'm}(J^*_p,\vec{K}_\alpha) = \frac{4\pi}{K_0}\sqrt{\frac{K_\alpha}{K_0}} \sum_{LL'J} (L0J_p m|Jm) \times e^{i[\omega_{L'}(\alpha)+\omega_L(0)]} (L'm - m'J^*_p m'|Jm) \times \widehat{\mathcal{T}}^J_{LJ_p:L'J^*_p}(K_\alpha) Y^0_L(\widehat{K}_0)\, Y^{m-m'}_{L'}(\widehat{K}_\alpha) \quad , \quad (18)$$

and similarly for the nuclear part of the elastic amplitude. It is usual to calculate these amplitudes in a coordinate system in which the x-axis is in the reaction plane of $\vec{K}_0$ and $\vec{K}_\alpha$. The CDCC scheme is available in a general coupled channels computer code [11].

C. Two-body scattering and breakup observables

The calculational structure outlined here leads to simple expressions for two-body scattering observables, such as the differential cross section angular distribution for elastic and inelastic scattering, and the inelastic scattering of the cm of p excited to a given bin. For elastic scattering, the diagonal point charge Coulomb amplitude must of course be added. The cm cross section angular distribution, summed over all included breakup excitations, is

$$\frac{d\sigma}{d\Omega_K} = \frac{1}{2J_p+1} \sum_{\alpha\neq 0, m'm} \left|\widehat{\mathcal{F}}_{m'm}(\alpha)\right|^2 \quad . \quad (19)$$

Similarly, from Eq.(18), one obtains the cross sections for each bin integrated over all directions of the emerging cm of the fragments, $d\sigma(J^*_p)/d\hat{\varepsilon}_i$.

D. Three-body breakup observables

Less obvious is the relationship of the CDCC two-body inelastic amplitudes $\widehat{\mathcal{F}}_{mm'}(\alpha)$ to the breakup transition amplitudes $T_m(\vec{k},\vec{K})$ from an initial state J_p, m to a general physical three-body final state of the constituents. This is needed to make predictions for experiments with general detection geometries, since each laboratory detector configuration and detected fragment energy involves a distinct final state cm wave vector $\vec{K}$, breakup energy ε_k, and relative motion wave vector $\vec{k}$.

Writing the CDCC approximation to the breakup transition amplitude by replacing Ψ^{CD} in an exact post-form matrix element, gives

$$T_m(\vec{k},\vec{K}) = \langle \phi^{(-)}_{\vec{k}}(\vec{r})\, e^{i\vec{K}\cdot\vec{R}} | U(\{\vec{R}_j\}) | \Psi^{CD}_{\vec{K}_0 m}(\vec{r},\vec{R}) \rangle \quad . \tag{20}$$

Inserting the set of bin-states, assumed complete for the model space used, then

$$T_m(\vec{k},\vec{K}) = \sum_{\alpha,m'} \langle \phi^{(-)}_{\vec{k}} | \hat{\phi}^{m'}_{\alpha} \rangle \langle \hat{\phi}^{m'}_{\alpha}, \vec{K} | U(\{\vec{R}_j\}) | \Psi^{CD}_{\vec{K}_0 m} \rangle \ . \tag{21}$$

We now recognise that the matrix elements $\widehat{\mathcal{F}}_{m'm}(\alpha)$, re-normalised to T-matrix normalisation by removal of the trivial two-body phase space factors, i.e.

$$\widehat{\mathcal{T}}_{m'm}(\alpha) = -\frac{2\pi\hbar^2}{\mu_p}\sqrt{\frac{K_0}{K_\alpha}}\,\widehat{\mathcal{F}}_{m'm}(\alpha) \quad , \tag{22}$$

are precisely the transition matrix elements

$$\widehat{\mathcal{T}}_{m'm}(\alpha) = \langle \hat{\phi}^{m'}_{\alpha}, \vec{K}_\alpha | U(\{\vec{R}_j\}) | \Psi^{CD}_{\vec{K}_0 m} \rangle, \tag{23}$$

obtained by coupled channels solution on a grid of θ_α and K_α values. In our spinless particle case, one finds

$$\langle \phi^{(-)}_{\vec{k}} | \hat{\phi}^{m'}_{\alpha} \rangle = \frac{(2\pi)^{3/2}}{k\sqrt{N_\alpha}} (-i)^\ell f_\alpha(k)\, e^{i[\delta_\ell(k)+\sigma_\ell(k)]} Y^{m'}_\ell(\hat{k}) \quad , \tag{24}$$

where $k \in \Delta k_\alpha$, and so

$$\begin{aligned} T_m(\vec{k},\vec{K}) \ &= \ \frac{(2\pi)^{3/2}}{k} \sum_{\ell m'} (-i)^\ell \, \exp(i[\delta_\ell(k)+\sigma_\ell(k)]) \\ &\times \ f_\alpha(k)\, Y^{m'}_\ell(\hat{k})\, T_{m'm}(\alpha,\vec{K}) \quad . \end{aligned} \tag{25}$$

In this equation the $T_{m'm}(\alpha,\vec{K})$ at the required final state vector $\vec{K} \equiv [K,\theta,\phi]$ can be obtained by interpolating the bracketed term on the right hand side of the expression

$$T_{m'm}(\alpha,\vec{K}) \leftarrow e^{i[m-m']\phi} \left[\widehat{\mathcal{T}}_{m'm}(\alpha)/\sqrt{N_\alpha} \right] \tag{26}$$

from the grid of calculated $[K_\alpha,\theta_\alpha]$ values.

The breakup triple differential cross section in the case of measurements of the energy of constituent 1, is

$$\frac{d^3\sigma}{dE_1 d\Omega_1 d\Omega_2} = \frac{2\pi\mu_p}{\hbar^2 K_0} \frac{1}{(2J_p+1)} \sum_m \left| T_m(\vec{k},\vec{K}) \right|^2 \rho_{12}, \tag{27}$$

where $\rho_{12} \equiv \rho(E_1,\Omega_1,\Omega_2)$ is the density of states for the frame (cm or laboratory) of interest [12].

E. Convergence considerations

The practical convergence of CDCC calculations of S-matrix elements and elastic scattering, transfer and breakup observables has been studied carefully for short-ranged U [7]. Convergence with respect to the included J_p^* channels, the potential multipole expansion, and k_{max} is readily tested. However, since the radial extent of the intrinsic bin states r_{bin} is proportional to $1/\Delta k_i$, a careful balance must be met between this maximum bin radius and the bin widths Δk_i, to ensure bin state normalisation, inclusion of the full bin strength and an accurate representation of the coupling interactions $V_{\alpha\beta}$ at large R.

The convergence of CDCC calculations for long ranged U, e.g. when including Coulomb breakup, has yet to be established [4]. The long range of U couples states close in the k continuum, requiring narrower bins, larger r_{bin}, and hence larger coupled channels sets. A problem has been the lack of an exact non-perturbative solution against which to assess this convergence. An alternative approach to Coulomb breakup is discussed in Section VII of these notes. This will be seen to yield a non-perturbative calculation of the Coulomb breakup amplitude without model space truncations or discretisation, which may aid an assessment of the CDCC convergence at higher energies.

V. ADIABATIC APPROXIMATION

A considerable simplification of the CDCC calculational scheme, permitting calculations for $n>2$, is achieved by use of an adiabatic treatment of the reaction dynamics. As for all adiabatic approximations, we must classify the dynamical variables into a high energy (*fast*) and a low energy (*slow*) set. In the present context we identify the energetic variable with $\vec{R}$, the projectile cm motion, and the slow variable with its internal motions $\vec{r}_i$. At high incident energy, to be quantified later, and for extended, weakly bound p, this division is very natural [13]. It is assumed therefore that the energies ε_k associated with the most strongly coupled excited configurations in Eq.(1), are such that $\varepsilon_k \ll E$; sometimes also referred as a sudden approximation. Equivalently, due to the slow internal motions of the constituents of p, the $\{\vec{r}_i\}$ are assumed frozen for the time taken for p to traverse the interaction region. This approximation is also the starting point for eikonal few-body approaches, based on impact parameter descriptions, discussed later in these notes.

Assuming $\varepsilon_k \ll E$, little error is made upon replacing H_p in Eq. (1) by a representative (small) constant energy. Furthermore, taking this energy as the projectile binding energy $-\varepsilon_0$, the adiabatic Schrödinger equation is, with $E_0 = E + \varepsilon_0$,

$$\left[T_R + U(\{\vec{R}_j\}) - E_0\right] \Psi^{AD}_{\vec{K}_0}(\{\vec{r}_i\}, \vec{R}) = 0 \tag{28}$$

whose solutions satisfy the required incident plane wave boundary conditions of Eq.(3) since their dominant elastic channel component has the correct channel energy. Clearly for $n=2$ Eq.(28) can be solved using the CDCC method, by calculating the coupled channels set, Eq.(12), with all $E_\alpha = E_0$. Indeed this provides a valuable check of numerical calculations. More importantly, the adiabatic approximation has removed the explicit dynamical dependence on the internal degrees of freedom of the projectile in Eq.(28), which is now an

effective two-body equation with only parametric dependence on the set $\{\vec{r}_i\}$. Its solution

$$\Psi^{AD}_{\vec{K}_0}(\{\vec{r}_i\},\vec{R}) = \psi^{AD}_{\vec{K}_0}(\{\vec{r}_i\},\vec{R})\phi^{(n)}_0(\{\vec{r}_i\}) \quad , \tag{29}$$

must be evaluated on a grid of required but fixed $\vec{r}_i$ values.

Except for the few-body wave function at coincidence ($\vec{r}_i$=0), the solution of Eq.(28) is obtained using coupled channels methods. At coincidence, however, Ψ^{AD} satisfies the one-body equation

$$\Big[T_R \,+\, U(\{\vec{R}\}) \,-\, E_0\Big]\, \Psi^{AD}_{\vec{K}_0}(0,\vec{R}) = 0 \quad . \tag{30}$$

The simplicity of this coincidence solution, and its deviation from the folding model solution due to V_{00}, Eq.(4), has provided great insight into the role of breakup effects in zero-range approximations to reaction amplitudes [8, 13].

In the general case, and for comparison with the CDCC methodology, we outline the structure of the adiabatic calculational scheme for Ψ^{AD} in the n=2 case. As for the CDCC analysis, we neglect particle spins. The method, including spin considerations, has also been applied for n=3 projectiles [14].

A. Adiabatic coupled equations solution

An accepted method of solution [15] is to make a truncated orbital angular momentum expansion in the internal coordinate $\vec{r}$, and hence to solve for the effective Hamiltonian

$$\mathcal{H}^{AD} = \mathcal{P}\mathcal{H}_0\mathcal{P}, \qquad \mathcal{P} = \sum_{\ell=0,m}^{\ell_{max}} |\ell m\rangle\langle \ell m|, \tag{31}$$

as a coupled channels problem. Here $\mathcal{H}_0 = T_R + U(\{\vec{R}_j\})$ is the adiabatic Hamiltonian. The generalisation, for n=3, is to truncate the angular momentum expansions for both of the internal coordinates [14].

The coupled equations can be set up by making the partial wave expansion of the scattering wavefunction,

$$\Psi^{AD}_{\vec{K}_0 m}(\vec{r},\vec{R}) = \sum_{JM_JL\ell} C^{JM_J}_{L\ell m}(\vec{K}_0, r)\Psi^{AD}_{JM_JL\ell}(\vec{r},\vec{R}), \tag{32}$$

where we assume the projectile is incident in the ground state, with angular momentum projection m, (and $J_p = \ell_0$)

$$\phi^{(2)}_0(\vec{r}) \equiv \phi^m_{\ell_0}(\vec{r}) = [u_{\ell_0}(r)/r]\, Y^m_{\ell_0}(\hat{r}) \quad . \tag{33}$$

The total angular momentum states are now

$$\begin{aligned}\Psi^{AD}_{JM_JL\ell}(\vec{r},\vec{R}) \;&= \sum_{L'M'\ell'm'} (L'M'\ell'm'|JM_J) i^{L'}\, Y^{M'}_{L'}(\hat{R}) \\ &\times\; Y^{m'}_{\ell'}(\hat{r})\, [\chi^J_{L\ell:L'\ell'}(r,R)/R],\end{aligned} \tag{34}$$

and the radial distorted waves χ^J, for each fixed r, satisfy the coupled radial equations

$$[E_0 - T_{L'}]\,\chi^J_{L\ell:L'\ell'}(r,R) = \sum_{\ell'' L''} i^{L''-L'} \times \langle (L'\ell')J||U(\{\vec{R}_j\})||(L''\ell'')J\rangle\, \chi^J_{L\ell:L''\ell''}(r,R) \tag{35}$$

subject to the boundary conditions

$$\chi^J_{L\ell:L'\ell'} \to F_{L'}(K_0R)\delta_{\ell'\ell}\delta_{L'L} + \mathcal{T}^J_{L\ell:L'\ell'}(r)H^+_{L'}(K_0R). \tag{36}$$

Here T_L is the kinetic energy operator in partial wave L and the partial wave $\mathcal{T}^J$ are now explicitly r dependent. In the coupling interactions in Eq.(35),

$$\langle \hat{R},\hat{r}|(L\ell)JM_J\rangle = \sum_{Mm}(LM\ell m|JM_J)\,Y^M_L(\hat{R})Y^m_\ell(\hat{r}), \tag{37}$$

and the bra-ket denotes integration over $\hat{R}$ and $\hat{r}$.

The coefficients C are once again obtained by matching to the entrance channel boundary condition. In this case

$$\begin{aligned} C^{JM_J}_{L\ell m}(\vec{K}_0,r) &= \frac{4\pi}{K_0 r}\sum_M e^{i\omega_L(0)}(LM\ell m|JM_J) \\ &\times\ Y^M_L(\hat{K}_0)^* u_{\ell_0}(r)\delta_{\ell\ell_0} \end{aligned} \tag{38}$$

The truncations required in this solution are (i) the order of the potential multipole expansion, and (ii) the maximum relative orbital angular momentum included ℓ_{max}. The convergence of the model calculations with respect to these parameters is readily established.

B. Elastic and inelastic scattering

It follows that the amplitude of the outgoing waves in Ψ^{AD}, in direction $\vec{K}$, when the projectile is incident with angular momentum projection m and a *fixed* spatial configuration $\vec{r}$, is

$$\begin{aligned} \mathcal{F}_m(\vec{r},\vec{K}) &= \frac{4\pi}{K_0 r}\sum_{LL'\ell'm'J}(L0\ell_0 m|Jm)e^{i[\omega_{L'}(0)+\omega_L(0)]} \\ &\times\ (L'm-m'\ell'm'|Jm)Y^0_L(\widehat{K}_0)\,Y^{m-m'}_{L'}(\widehat{K}) \\ &\times\ \mathcal{T}^J_{L\ell_0:L'\ell'}(r)Y^{m'}_{\ell'}(\hat{r})u_{\ell_0}(r)\quad , \end{aligned} \tag{39}$$

with $|\vec{K}| = K_0$. The predictions for elastic or inelastic scattering can now be obtained by direct overlap with the appropriate final state,

$$F_{m'm}(\vec{K}) = \langle \phi^{m'}_i|\mathcal{F}_m(\vec{K})\rangle, \tag{40}$$

where the integral is over $\vec{r}$. For inelastic scattering to a bound excited state with orbital angular momentum ℓ_1, Eq.(33), then

$$\begin{aligned} F_{m'm}(\vec{K}) &= \frac{4\pi}{K_0}\sum_{LL'J}(L0\ell_0 m|Jm)e^{i[\omega_{L'}(0)+\omega_L(0)]} \\ &\times (L'm-m'\ell_1 m'|Jm)Y_L^0(\widehat{K}_0)\,Y_{L'}^{m-m'}(\widehat{K}) \\ &\times \int_0^\infty dr\, u_{\ell_1}^*(r)\mathcal{T}^J_{L\ell_0:L'\ell_1}(r)u_{\ell_0}(r) \quad . \end{aligned} \tag{41}$$

For elastic scattering, one must add the point Coulomb amplitude $f_C^{pt}(\theta)$ and of course $\ell_1=\ell_0$. For $\ell_0=0$ we have

$$\begin{aligned} F(\vec{K}) &= f_C^{pt}(\theta)+\frac{1}{K_0}\sum_L(2L+1)e^{2i\omega_L(0)}P_L(\cos\theta) \\ &\times \int_0^\infty dr\,|u_0(r)|^2\mathcal{T}^L_{L0:L0}(r) \quad , \end{aligned} \tag{42}$$

where θ is the scattering angle.

C. Breakup reactions

Since the projectile ground state $\phi_0^{(n)}$ is a factor in the adiabatic wavefunction, Eq.(29), it is clear that at large constituent particle separations, $\vec{r}_i\to\infty$, the solution will vanish in a region which should contain contributions from some parts of the breakup flux. So, for large r_i, Ψ^{AD} will certainly be inaccurate. This is a consequence of our assumption that the entire spectrum of H_p is degenerate with the ground state. It follows that, to use Ψ^{AD} to calculate a breakup amplitude (for n=2) we must limit it to certain regions of the six-dimensional ($\vec{r}$,$\vec{R}$) space. For instance, breakup channel overlaps $\langle\phi^{(-)}_{\vec{k}}|\mathcal{F}_m(\vec{K})\rangle$, analogous to Eq.(40), would probe the adiabatic wavefunction in areas where it is known to be incorrect and so we cannot extract the breakup amplitude directly from the asymptotics of the adiabatic solution.

In applications [16] to breakup reactions, Ψ^{AD} has therefore been used in the post form breakup transition matrix element

$$T_m(\vec{k},\vec{K})=\langle\phi^{(-)}_{\vec{k}}(\vec{r})\,e^{i\vec{K}\cdot\vec{R}}|U(\{\vec{R}_j\})|\Psi^{AD}_{\vec{K}_0 m}(\vec{r},\vec{R})\rangle \quad , \tag{43}$$

discussed in connection with the CDCC method. This matrix element is a natural choice given the ($\vec{r}$,$\vec{R}$) coordinate representation of Ψ^{AD}. Calculation of this matrix element requires the few-body wavefunction only in the interaction region of U and the contributions from large r are de-emphasised in the calculation of the largest components of the breakup reaction.

It is important to recall also that incorporating the adiabatic wavefunction, and evaluating such a breakup amplitude, constitutes an iteration beyond the lowest-order adiabatic method. Formally, calculation of Eq.(43) is equivalent to extracting the required amplitudes from the asymptotics of the solution of the inhomogeneous equation

$$[E-T_R-H_p]\,\Psi_{\vec{K}_0}(\vec{r},\vec{R})=U(\{\vec{R}_j\})\Psi^{AD}_{\vec{K}_0}(\vec{r},\vec{R}), \tag{44}$$

in which Ψ^{AD} appears only in the source term. While the calculation of Ψ^{AD} neglects the projectile excitation energy, the bra in the calculation of T_m includes correctly the final state wavefunctions, kinematics and excitation energies. The calculation does not therefore make the zero adiabaticity parameter ($\xi = 0$) approximation of semi-classical theories [4]. We return to this point in discussing the recoil approximation to the adiabatic calculation in Section VII.

The adiabatic approximation can also be used to provide an approximate few-body wavefunction in reaction channels, such as involve the pp and d* (spin singlet np) two-body systems, in which there is no bound state. Applications of this type include the (^{3}He,pp) [17] and (p,d*) [18] transfer reactions to these unbound continuum final states.

D. Convergence and accuracy

The adiabatic approximation assumes the states of H_p excited are of low energy. Of course the strengths with which the spectrum of breakup states of H_p are actually excited in a collision will be dictated by the magnitudes, and moreover the geometries, of the tidal forces experienced by the projectile's constituents. It is the radius and surface diffuseness of the V_{jt} which dictate the strong differential forces exerted on the constituents at the nuclear surface. For excitation due to the strong interaction, where the optical potentials V_{jt} have surface diffuseness parameters of order 1 fm, the excitation energy spectrum (calculated using the CDCC) typically extends to 10's of MeV. For a long range interaction with slow spatial variation, the V_{jt} couple states of H_p only in close proximity in relative energy. Since the important surface diffuseness of nuclear optical potentials is essentially constant with nuclide and incident energy, the adiabatic approximation becomes increasingly good at sufficiently high energies.

This validity has been studied extensively for elastic and breakup reactions in deuteron, ^{6}Li, and ^{7}Li induced reactions [7] and found to lead to good agreement with the CDCC for projectile energies in excess of $\approx$50 MeV/nucleon. For elastic and inelastic excitations the relevant amplitudes, Eq.(40), sample the few-body wavefunction over the range of the ground or excited state. These are principally sensitive to the low ε_k components in the wavefunction, for which the adiabatic approach is well suited. For transfer reactions, however, the cross section angular distributions are almost always a delicate interference of the contributions from transfers taking place on the near- and far-sides of the nucleus and, particularly with increasing energy and momentum mismatch in the reaction, are sensitive to different parts of the excited spectrum in the few-body wavefunction [8, 19]. This results in a far greater sensitivity to the higher ε_k components in the wavefunction [19] which are less well represented in the adiabatic limit. Numerous non-adiabatic extensions have been proposed [8, 20] to improve the description of these breakup components of high relative momenta. One of the simplest of these, the quasi-adiabatic approach, is outlined very briefly in the following Section. In general, in applications to transfer reactions, corrections to the adiabatic theory need to be examined. The CDCC method is of course also applicable.

VI. QUASI-ADIABATIC APPROXIMATION

Quasi-adiabatic methods remove the degeneracy of the elastic and continuum channels, assumed in the adiabatic calculation of the n-body wavefunction, while at the same time retaining much of the simplicity of the adiabatic theory [21]. They do so by introducing a representative continuum energy $\bar{\varepsilon} \neq -\varepsilon_0$ for the entire spectrum of breakup states of the projectile, which may however depend on the cm position coordinate and partial wave L [21, 22].

From the adiabatic wavefunction calculated using the coupled channels approach of this Section, the elastic and breakup channels components of the solution can be separated by projection,

$$\psi^{AD,el}_{\vec{K}_0}(\vec{R}) = \langle \phi^{(n)}_0 | \Psi^{AD}_{\vec{K}_0} \rangle, \tag{45}$$

and subtraction

$$\psi^{AD,bu}_{\vec{K}_0}(\{\vec{r}_i\},\vec{R}) = \psi^{AD}_{\vec{K}_0}(\{\vec{r}_i\},\vec{R}) - \psi^{AD,el}_{\vec{K}_0}(\vec{R}). \tag{46}$$

Decomposing similarly the original, non-adiabatic, Schrodinger equation

$$\begin{aligned} \Big[T_R \,+\, U(\{\vec{R}_j\}) \,+\, H_p - E\Big]\, \Psi^{bu}_{\vec{K}_0}(\{\vec{r}_i\},\vec{R}) \\ = \,\Big[E_0 - T_R - U(\{\vec{R}_j\})\Big]\, \Psi^{el}_{\vec{K}_0}(\vec{R}), \end{aligned} \tag{47}$$

the quasi-adiabatic approximation solves this inhomogeneous problem by replacing (i) $H_p \rightarrow \bar{\varepsilon}$ on the left hand side, and (ii) $\Psi^{el} \rightarrow \Psi^{AD,el}$ in the evaluation of the source term. That is

$$\begin{aligned} \Big[\, T_R \,+\, U(\{\vec{R}_j\}) \,+ \bar{\varepsilon} - \,E\Big]\, \psi^{QAD,bu}_{\vec{K}_0}(\{\vec{r}_i\},\vec{R}) \\ = \,\Big[U^{AD}_{opt}(\vec{R}) - U(\{\vec{R}_j\})\Big]\, \psi^{AD,el}_{\vec{K}_0}(\vec{R}) \quad , \end{aligned} \tag{48}$$

where U^{AD}_{opt} is the local equivalent potential to the adiabatic elastic component $\Psi^{AD,el}$. Similar expressions can be written down at the partial wave level. In applications, $\bar{\varepsilon}$ can be taken from the qualitative behaviour found from CDCC calculations [21] or, like the source term in Eq.(48), can be estimated from the adiabatic solution. For example, as the expectation value of H_p in the breakup states [22]

$$\bar{\varepsilon}(R) = \frac{\langle \Psi^{AD,bu}_{\vec{K}_0} | H_p | \Psi^{AD,bu}_{\vec{K}_0} \rangle}{\langle \Psi^{AD,bu}_{\vec{K}_0} | \Psi^{AD,bu}_{\vec{K}_0} \rangle}. \tag{49}$$

This value can also be used as a starting energy from which to iterate Eq.(48), subsequent iterations using $\bar{\varepsilon}$ computed instead from $\Psi^{QAD,bu}$. Applications of the quasi-adiabatic approach have clarified the importance of the high energy breakup components in transfer processes, and also shown that the approach provides a better description of these high energy components [8, 21, 22].

VII. RECOIL ADIABATIC APPROXIMATION

A very useful special case of the adiabatic model is obtained when the potential $V_{ct}(R_c)$, between just one of the projectile constituents c and the target, dominates in $U(\{\vec{R}_j\})$. We

refer to c as the projectile core. So, $\vec{R}_c = \vec{R} - \gamma_c \vec{r}$, where $\vec{r}$ is the position of the cm of the remaining $n-1$ *valence* particles v relative to c, and $\gamma_c = 1 - m_c/m_p$. In this limit we show that there is an exact closed form solution $\bar{\Psi}^{AD}$ of the adiabatic $n+1$-body Schrödinger equation [23] which satisfies

$$[\, T_{\vec{R}} \, + \, V_{ct}(R_c) \, - \, E_0] \, \bar{\Psi}^{AD}_{\vec{K}_0}(\{\vec{r}_i\}, \vec{R}) = 0 \quad . \tag{50}$$

It follows that excitation of the projectile or removal of the valence particles v is by virtue only of the interaction and recoil of the core, also referred to as a 'shake-off' mechanism. Applications of this limit include the scattering of halo nuclei [24] such as ^{11}Be, described as a heavy core nucleus ^{10}Be bound to a single valence neutron by only 0.5 MeV. Here the ^{10}Be core-target potential is much stronger, and of longer range, than the neutron-target potential, i.e. $V_{ct} \gg V_{vt}$. The scattering of a composite projectile from a highly charged target, when only the projectile core is charged, is another very important case [25] discussed in the following.

As well as providing physical insight, the recoil limit is valuable for providing a detailed test of the computational and numerical coupled channels methods, since coupled channels solution, orbital angular momentum truncation, and multipole expansion and truncation are unnecessary in this case.

A. Recoil limit solution

To solve the recoil limit Schrödinger equation, Eq.(50), we introduce the translation operator $U(\vec{x})$, which shifts the cm variable $\vec{R}$ through $-\vec{x}$, i.e. $U(\vec{x}) = \exp(-\vec{x} \cdot \nabla_R)$. Since the potential operator V_{ct} is

$$V_{ct}(\vec{R}_c) = U(\gamma_c \vec{r}) V_{ct}(\vec{R}) U^\dagger(\gamma_c \vec{r}) \quad , \tag{51}$$

and $[U(\gamma_c \vec{r}), \nabla^2_R] = 0$, then

$$\left[T_R \, + \, V_{ct}(\vec{R}) \, - \, E_0 \right] \left(U^\dagger(\gamma_c \vec{r}) \bar{\Psi}^{AD}_{\vec{K}_0}(\{\vec{r}_i\}, \vec{R}) \right) = 0 \quad . \tag{52}$$

Evidently, the most general form of the solution $U^\dagger \bar{\Psi}$ of this equation is the product of an arbitrary function $\mathcal{F}(\vec{r})$ of the separation of c and v, the projectile ground state $\phi_0^{(n)}$ and a projectile cm distorted wave $\chi^{(+)}(\vec{R})$,which satisfies the one-body Schrödinger equation

$$\left[T_R \, + \, V_{ct}(\vec{R}) \, - \, E_0 \right] \chi^{(+)}_{\vec{K}_0}(\vec{R}) = 0 \quad . \tag{53}$$

In the present context therefore $\chi^{(+)}$ is the distorted wave which describes the scattering of the projectile, considered point-like, by the core interaction V_{ct}. The required many-body solution of Eq.(50) is therefore

$$\begin{aligned} \bar{\Psi}^{AD}_{\vec{K}_0}(\{\vec{r}_i\}, \vec{R}) \; &= \; \mathcal{F}(\vec{r}) \left[U(\gamma_c \vec{r}) \chi^{(+)}_{\vec{K}_0}(\vec{R}) \right] \phi_0^{(n)}(\{\vec{r}_i\}) \\ &= \; \mathcal{F}(\vec{r}) \chi^{(+)}_{\vec{K}_0}(\vec{R}_c) \phi_0^{(n)}(\{\vec{r}_i\}) \quad , \end{aligned} \tag{54}$$

where $\chi^{(+)}$ is evaluated at the core's position coordinate $\vec{R}_c$. We note that, since $[U(\gamma_c\vec{r}), H_p] \neq 0$, this product solution follows from Eq.(1), with $U = V_{ct}$, only if H_p is treated adiabatically.

The multiplicative function $\mathcal{F}$, chosen to satisfy the incident wave boundary condition, Eq.(3), is

$$\mathcal{F}(\vec{r}) = \exp(i\gamma_c \vec{K}_0 \cdot \vec{r}), \tag{55}$$

and the *exact* solution of the adiabatic problem, Eq.(50), is

$$\bar{\Psi}^{AD}_{\vec{K}_0}(\{\vec{r}_i\}, \vec{R}) = \exp(i\gamma_c \vec{K}_0 \cdot \vec{r}) \chi^{(+)}_{\vec{K}_0}(\vec{R}_c) \phi^{(n)}_0(\{\vec{r}_i\}) \quad . \tag{56}$$

It is important to stress that this wavefunction retains break-up components and excitations to any bound excited states. These couplings are manifest in the complex dependence of the wavefunction on $\vec{r}$ through both $\chi^{(+)}$ and the exponential factor.

The asymptotic form of the wavefunction for large R in direction $\vec{K}$, and finite r_i, is

$$\bar{\Psi}^{AD}_{\vec{K}_0}(\{\vec{r}_i\}, \vec{R}) \to \phi^{(n)}_0(\{\vec{r}_i\}) e^{i\gamma_c \vec{q}\cdot\vec{r}} f_{pt}(\vec{K}_0, \vec{K}) \frac{e^{iKR}}{R}, \tag{57}$$

with $|\vec{K}| = |\vec{K}_0|$. Here $\vec{q} = \vec{K}_0 - \vec{K}$ is the momentum transfer in the reaction, and $f_{pt}(\vec{K}_0, \vec{K})$ the point projectile elastic scattering amplitude associated with $\chi^{(+)}$.

B. Elastic and inelastic scattering

Elastic and inelastic scattering in the recoil adiabatic limit is, replacing $\Psi^{(+)}$ by $\bar{\Psi}^{AD}$ in the transition amplitude

$$\bar{T}(\vec{K}_\alpha) = \langle \phi^{(n)}_\alpha(\{\vec{r}_i\})\, e^{i\vec{K}_\alpha\cdot\vec{R}} | V_{ct} | \Psi^{(+)}_{\vec{K}_0}(\{\vec{r}_i\}, \vec{R}) \rangle \quad , \tag{58}$$

given by the factorisation

$$\begin{aligned} \bar{T}(\vec{K}_\alpha) &= \langle \phi^{(n)}_\alpha | e^{i\gamma_c\vec{q}\cdot\vec{r}} | \phi^{(n)}_0 \rangle \, \langle \vec{K}_\alpha | V_{ct} | \chi^{(+)}_{\vec{K}_0} \rangle \\ &= F_{\alpha 0}(\gamma_c \vec{q})\, T_{pt}(\vec{K}_0, \vec{K}_\alpha). \end{aligned} \tag{59}$$

If, in keeping with the adiabatic approximation, we assume $|\vec{K}_\alpha| = |\vec{K}_0|$, this result can also be obtained from the asymptotic form, Eq.(57). Then T_{pt} is the elastic scattering transition amplitude describing the scattering of p, assumed point-like, by V_{ct}. The formfactor $F_{\alpha 0}$ accounts fully for the effects of projectile structure and excitation. If in Eq.(58) we take $|\vec{K}_\alpha| \neq |\vec{K}_0|$ then T_{pt} must be calculated half-off the energy shell. This poses a problem in situations where the Coulomb interaction plays a significant role due to the singular nature of the half-off-shell Coulomb T-matrix.

The corresponding scattering differential cross sections are

$$\left(\frac{d\sigma}{d\Omega}\right)_\alpha = |F_{\alpha 0}(\gamma_c\vec{q})|^2 \ \left(\frac{d\sigma}{d\Omega}\right)_{pt} \quad . \tag{60}$$

Clearly T_{pt} can be highly constrained if experimental data on the elastic scattering of the core from the target is available to determine V_{ct}. The importance of Eq.(60) is that it then identifies those scattering angles and incident energies at which the structure of a loosely-bound projectile, with a given wavefunction, will be manifest as a deviation from the scattering expected if it were a point projectile [23].

While the formfactor in Eq.(60) is also reminiscent of factorisations which occur when using Born approximation and approximate distorted wave theories, the analysis which led to this result does not involve such approximations. In fact, only when all intermediate states are included do the second- and higher-order terms in the Born series for the amplitude factorise in this way. The same argument pertains for the factorisation of the wavefunction in Eq.(56).

C. Breakup reactions

Eq.(56) is the exact solution of our stated few-body model, given only the adiabatic assumption. The explicit form again makes clear that, for large r, $\bar{\Psi}$ will be inaccurate. The appropriate breakup matrix element must be chosen accordingly. As for the elastic and inelastic channels, we can write

$$\bar{T}(\vec{k},\vec{K}) = \langle \phi^{(-)}_{\vec{k}}(\vec{r})\, e^{i\vec{K}\cdot\vec{R}} | V_{ct}(R_c) | \bar{\Psi}^{(+)}_{\vec{K}_0}(\vec{r},\vec{R}) \rangle \quad , \tag{61}$$

and achieve a similar factorisation

$$\bar{T}(\vec{k},\vec{K}) = F_{\vec{k}0}(\gamma_c\vec{q})\, T_{pt}(\vec{K}_0,\vec{K}), \tag{62}$$

where now $F_{\vec{k}0}(\gamma_c\vec{q}) = \langle \phi^{(-)}_{\vec{k}} | e^{i\gamma_c\vec{q}\cdot\vec{r}} | \phi_0 \rangle$. While this amplitude may be reasonable for a short ranged V_{ct}, when V_{ct} is of long range the integrand in Eq.(61) is not restricted to small r. The problem with the half-off-shell T_{pt} for the Coulomb interaction also remains with this matrix element.

Since however the distorted wave appearing in Eq.(56) for $\bar{\Psi}^{AD}$ is now a function of $\vec{R}_c$, then an alternative breakup transition amplitude is (with n=2 for simplicity)

$$\tilde{T}(\vec{K}_v,\vec{K}_c) = \langle e^{i\vec{K}_v\cdot\vec{R}_v}\, \chi^{(-)}_{\vec{K}_c}(\vec{R}_c)\, |V_{vc}|\, \bar{\Psi}^{AD}_{\vec{K}_0}(\vec{r},\vec{R}) \rangle \ . \tag{63}$$

This is the breakup amplitude to a c+v final state with core momentum $\vec{K}_c = (1-\gamma_c\gamma_{tc})\vec{K} - \gamma_{tc}\vec{k}$ and valence particle momentum $\vec{K}_v = \gamma_c\vec{K} + \vec{k}$ in the cm frame, where $\gamma_{tc} = m_t/(m_c + m_t)$. $\chi^{(-)}$ is the final state wavefunction of the core, distorted by V_{ct}. Since $V_{vt} = 0$, the valence particle's final state is a plane wave. Due to the short range of $V_{vc} \equiv V_{vc}(\{\vec{r}_i\})$, the sum of all interactions internal to H_p, the integrand in Eq. (63) involves only finite $\vec{r}_i$ irrespective of the range of V_{ct}.

As in our discussion of Eq.(44), evaluation of $\tilde{T}$ is equivalent to solving the inhomogeneous problem

$$[E - T_v - T_c - V_{ct}]\, \Psi_{\vec{K}_0}(\vec{r},\vec{R}) = V_{vc}(\vec{r})\bar{\Psi}^{AD}_{\vec{K}_0}(\vec{r},\vec{R}) \quad , \tag{64}$$

where T_v and T_c are the valence and core particle kinetic operators. It goes beyond the lowest order adiabatic approximation since it includes correctly the final state wavefunctions, kinematics and excitation energies.

Substituting Eq.(56) in $\tilde{T}$, and noting that $\vec{R}_v = \gamma_{tc}\vec{R}_c + \vec{r}$, the breakup amplitude is once again seen to factorise *exactly* as

$$\tilde{T}(\vec{K}_v, \vec{K}_c) = \langle \vec{P}_v | V_{vc} | \phi_0 \rangle \ \langle \vec{Q}_v, \chi^{(-)}_{\vec{K}_c} | \chi^{(+)}_{\vec{K}_0} \rangle \quad , \tag{65}$$

where we have introduced momenta $\vec{P}_v = \vec{K}_v - \gamma_c \vec{K}_0$ and $\vec{Q}_v = \gamma_{tc}\vec{K}_v$. The two factors delineate the structure and dynamical parts of the calculation.

The projectile structure enters through the first term, the vertex function $\langle \vec{P}_v | V_{vc} | \phi_0 \rangle$ which can be evaluated given a structure model for the projectile. This matrix element reflects the fact that, in the recoil ($V_{vt} = 0$) limit, momentum can be transferred to the valence particle only by virtue of its interaction V_{vc} with the core. Since $\gamma_c \vec{K}_0$ is the fraction of the projectile momentum carried by the incident valence particle, $\vec{P}_v$ is the momentum transfer to the valence particle. The vertex displays explicitly this momentum transfer from the ground state via V_{vc}.

The second term contains all the dynamics of the breakup process. In general this overlap of the three continuum functions $\langle \vec{Q}_v, \chi^{(-)}_{\vec{K}_c} | \chi^{(+)}_{\vec{K}_0} \rangle$ is difficult to evaluate, though it can be handled using the Vincent-Fortune integration procedure [26]. It can however be evaluated in closed form, and expressed in terms of the bremsstrahlung integral [27], when V_{ct} is the Coulomb interaction and the distorted waves are three-dimensional Coulomb waves. This limit has been applied to study the Coulomb breakup of both n=2 [25] and n=3 [28] projectiles.

Eq.(65) is also significant since it treats exactly the finite-range nature of the interaction V_{vc}, unlike zero-range and local energy approximations [2]. The amplitude is therefore applicable to projectiles with any ground state orbital angular momentum structure, and also includes breakup contributions from all interaction multipoles and relative orbital angular momenta between the valence and core fragments. The amplitude goes significantly beyond DWBA theories since it includes the initial and final state interactions V_{ct} and V_{vc} to all orders.

In conclusion, the recoil adiabatic limit provides a closed form solution of the few-body problem which becomes more accurate with increasing incident energy. It thus provides a valuable check of truncated calculational schemes, such as those discussed in Sections IV and V, and also of the (more approximate) impact parameter approaches of the subsequent Sections.

VIII. EIKONAL POINT-PARTICLE SCATTERING

In practice, the approaches discussed so far have been restricted to projectiles modeled as two- or three-body systems. Indeed, only the adiabatic and recoil adiabatic models have been used with a three-body projectile [14, 28]. A more efficient approach for dealing with an n-body projectile, the few-body Glauber (FBG) model, is based on the eikonal approximation. Provided that certain conditions hold, the FBG approach can also be the most

efficient method for dealing with three- and four-body systems, even when other approaches are applicable. We first introduce the ideas behind the eikonal and more general impact parameter descriptions using the scattering of a point projectile from a target. We then extend the approach to treat the scattering of composite systems.

A. The eikonal approximation

The eikonal approximation was introduced in quantum scattering theory by Moliere and later developed by Glauber. It was Glauber who applied it to nuclear scattering where he formulated a many-body, multiple scattering generalisation of the method [29]. We first describe the eikonal approximation as applied to non-relativistic point particle scattering from a central potential $V_{pt}(R)$.

In common with other semi-classical approaches, the eikonal method is useful when the wavelength of the incident particle is short compared with the distance over which the potential varies appreciably. This short wavelength condition is expressed in terms of the incident centre of mass wave number, K_0, and the range of the interaction, R_0, such that

$$K_0 R_0 \gg 1 \ . \tag{66}$$

However, unlike short wavelength methods such as the WKB approximation, the eikonal approximation also requires high scattering energies, such that

$$E \gg |V_0| \ , \tag{67}$$

where V_0 is a measure of the strength of the potential. In practice, and when V_{pt} is complex, this high energy condition is not critical and the eikonal approximation works well even when $E \approx |V_0|$ provided the first condition, Eq.(66), holds and we restrict ourselves to forward angle scattering.

Since the potential varies slowly on the length scale of the incident wavelength, it is reasonable to extract the free incident plane wave from the scattering wave function as a factor, i.e.

$$\psi^{(+)}_{\vec{K}_0}(\vec{R}) = e^{i\vec{K}_0\cdot\vec{R}}\,\omega(\vec{R}) \ , \tag{68}$$

where $\omega(\vec{R})$ is a, as yet unspecified, modulating function. The eikonal approximation to $\psi^{(+)}$ can be derived starting from either the Schrödinger equation or the Lippmann-Schwinger equation. Here we follow the first approach. The scattering wave function of Eq.(68) is substituted in the Schrödinger equation

$$\left[\nabla^2_R + K_0^2 - \frac{2\mu_p}{\hbar^2}V_{pt}\right]\ e^{i\vec{K}_0\cdot\vec{R}}\ \omega(\vec{R}) = 0 \ , \tag{69}$$

where μ_p is the reduced mass. Using the eikonal conditions, of Eqs.(66) and (67) and with the coordinate z-axis along the incident wave vector $\vec{K}_0$, Eq.(69) reduces to the first order equation for ω

$$\frac{\partial\omega}{\partial z} = -\frac{i\mu_p}{\hbar^2 K_0}\,V_{pt}\omega \ . \tag{70}$$

The solution of this equation, with the incident wave boundary condition requirement that $\omega(z \to -\infty) = 1$, is

$$\omega(\vec{R}) = \exp\left\{-\frac{i\mu_p}{\hbar^2 K_0}\int_{-\infty}^{z} V_{pt}(x,y,z')dz'\right\}, \tag{71}$$

and yields the eikonal approximation to the wave function

$$\psi^{eik}_{\vec{K}_0}(\vec{R}) = \exp\left\{i\vec{K}_0\cdot\vec{R} - \frac{i}{\hbar v}\int_{-\infty}^{z} V_{pt}(x,y,z')dz'\right\}, \tag{72}$$

where $v = \hbar K_0/\mu_p$ is the classical incident velocity in the cm frame. Thus, the modulating function introduces a modification to the phase of the incident plane wave. This modification involves an integration along the direction of the incident beam and, as such, assumes that the effects of V_{pt} are accurately accounted for by assuming the projectile traverses a straight line path. The eikonal method is therefore more accurate at forward scattering angles.

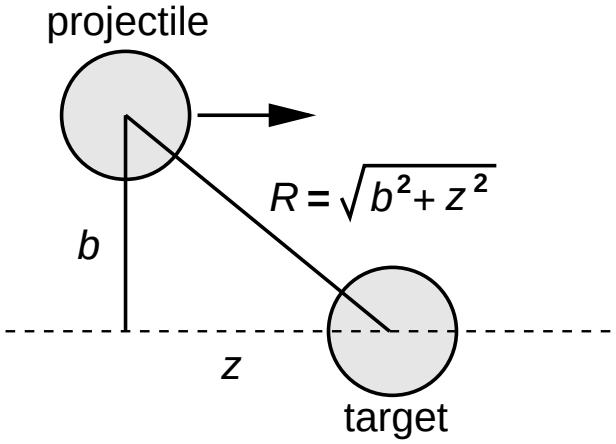

FIG.3 The straight line trajectory assumption of the eikonal approximation.

The eikonal wavefunction has incorrect asymptotics and so, to calculate amplitudes and observables, must be used within a transition amplitude. Thus, starting from the exact elastic transition amplitude

$$T(\vec{K}_0,\vec{K}) = \langle\vec{K}|\ V_{pt}\ |\psi^{eik}_{\vec{K}_0}\rangle\ , \tag{73}$$

the eikonal approximation to the elastic scattering amplitude is

$$f_0(\vec{K}) = -\frac{\mu_p}{2\pi\hbar^2}\int d\vec{R}\ \ e^{i\vec{q}\cdot\vec{R}}\ \ V_{pt}(R)\,\omega(\vec{R})\ , \tag{74}$$

where $\vec{q} = \vec{K}_0 - \vec{K}$ is the momentum transfer. We shall use a subscript zero throughout to denote quantities calculated in the eikonal limit. Since $|\vec{K}| = |\vec{K}_0|$, then for small forward angles, $\vec{q}$ is almost perpendicular to $\vec{K}_0$. In cylindrical polar coordinates,

$$\vec{R} = \vec{b} + \widehat{K}_0 z = \vec{b} + \vec{z}\ , \tag{75}$$

where $\vec{b}$ is the impact parameter, Figure 3, which lies in the x–y plane. Thus we have

$$\vec{q}\cdot\vec{R} = \vec{q}\cdot\vec{b} + \vec{q}\cdot\vec{z} \approx \vec{q}\cdot\vec{b}\ . \tag{76}$$

In addition, the product $V_{pt}\omega$ is known from Eq.(70) and when substituted in Eq.(74) gives

$$\begin{aligned} f_0(\vec{K}) &= -\frac{iK_0}{2\pi}\int d\vec{b}\, e^{i\vec{q}\cdot\vec{b}}\int_{-\infty}^{\infty} dz\ \frac{\partial\omega}{\partial z} \\ &= -\frac{iK_0}{2\pi}\int d\vec{b}\, e^{i\vec{q}\cdot\vec{b}}\left(e^{i\mathcal{X}_0(b)} - 1\right), \end{aligned} \tag{77}$$

where the eikonal phase shift function, $\mathcal{X}_0(b)$, is

$$\mathcal{X}_0(b) = -\frac{1}{\hbar v}\int_{-\infty}^{\infty} V_{pt}(R)\ dz\ . \tag{78}$$

Since we are assuming a central potential, f_0 will also possess azimuthal (cylindrical) symmetry. The azimuthal angle integration in Eq.(77) can therefore be carried out giving the more familiar form

$$f_0(\theta) = -iK_0\int_0^{\infty} b\, db\, J_0(qb)\,[\mathcal{S}_0(b) - 1]\ , \tag{79}$$

where $q = 2K_0\sin(\theta/2)$, θ is the scattering angle, and $\mathcal{S}_0(b) = \exp[i\mathcal{X}_0(b)]$ is the eikonal elastic S-matrix element at impact parameter b.

One can obtain the same expression for the elastic scattering amplitude by choosing the z-axis to be along the bisector of the incoming and outgoing momenta, $\vec{K}_0$ and $\vec{K}$. With this choice, we have $\vec{q}\cdot\vec{R} = \vec{q}\cdot\vec{b}$ exactly and so there are no small angle restrictions in the amplitude. However, it should be remembered that the z-direction was originally chosen to be along $\vec{K}_0$ in the wave function which enters the derivation of the amplitude in Eq.(73)

B. Coulomb interactions

In deriving $\mathcal{X}_0(b)$ above, it was implicit that $V_{pt}(R)$ was such that Eq.(78) converges. This is certainly the case for a short range strong nuclear interaction. When V_{pt} includes a Coulomb interaction then we obtain a sum of phase shifts $\mathcal{X}_0 = \mathcal{X}_{0N} + \mathcal{X}_{0C}$ of nuclear and Coulomb terms. Due however to the $1/R$ behaviour of V_C the Coulomb phase integral diverges logarithmically and a screening radius, a, must be introduced to shield the charge at large distances. This screening affects the scattered intensity only at scattering angles $\theta_C < (K_0 a)^{-1}$. Since a is typically of atomic dimensions, for the incident energies of interest the angle θ_C is much smaller than any at which measurements are made. For angles $\theta \gg \theta_C$ we observe particles whose impact parameters $b \ll a$ and the Coulomb phase shift can be written [29] as a sum of terms, $\mathcal{X}_{0C} = \mathcal{X}_{0\rho} + \mathcal{X}_a$. The first term depends on the form of the assumed Coulomb interaction and $\mathcal{X}_a = -2\eta\ln(K_0 a)$ is a constant screening phase in which η is the Sommerfeld parameter. Thus the eikonal scattering amplitude for a screened Coulomb potential is

$$\bar{f}_0(\theta) = e^{i\mathcal{X}_a}\left\{f_C^{pt}(\theta) - iK_0\int_0^{\infty} b\, db\ \ J_0(qb)\, e^{i\mathcal{X}_{pt}}[\bar{\mathcal{S}}_0 - 1]\right\} \tag{80}$$

where f_C^{pt} is the Coulomb amplitude for point charge (Rutherford) scattering. The point Coulomb phase shift appearing in the eikonal term is $\mathcal{X}_{pt}(b) = 2\eta \ln(K_0 b)$. The Coulomb modified eikonal S-matrix $\bar{\mathcal{S}}_0(b)$ characterises the deviations from point Coulomb scattering and is

$$\bar{\mathcal{S}}_0(b) = \exp\left[i\mathcal{X}_{0N} \; + \; i\mathcal{X}_{0\rho} - i\mathcal{X}_{pt}\right] . \tag{81}$$

The screening affects the scattering amplitude only as an overall (constant) real phase $\mathcal{X}_a$ and has no consequence for calculated observables.

IX. NON-EIKONAL EXTENSIONS

In the previous Section an approximate form for the elastic scattering amplitude was derived within the eikonal model. However, the eikonal approximation is not necessary to write the scattering amplitude as an impact parameter integral. Consider the exact scattering amplitude, written as a partial wave sum,

$$F(\theta) = \frac{1}{2iK_0} \sum_{\ell=0}^{\infty} (2\ell+1)\, P_\ell(\cos\theta)\, [\mathcal{S}_\ell - 1] \; , \tag{82}$$

where $P_\ell(\cos\theta)$ is a Legendre polynomial. $\mathcal{S}_\ell = \exp(2i\delta_\ell)$ is the exact partial wave S-matrix element obtained by solution of the radial Schrödinger equation for a given orbital angular momentum ℓ in the presence of the assumed $V_{pt}(R)$. The amplitude F can, alternatively, be written as a continuous integral, a Fourier-Bessel expansion,

$$F(\theta) = -iK_0 \int_0^{\infty} b\, db\, J_0(qb)\, a(K_0, b) \; , \tag{83}$$

where the amplitude $a(K_0, b)$ is [30]

$$a(K_0, b) = \frac{1}{K_0 b} \sum_{\ell=0}^{\infty} (2\ell+1)\, J_{2\ell+1}(2K_0 b)\, [\mathcal{S}_\ell - 1]. \tag{84}$$

Eqs.(83) and (84) are exact and valid for all energies and angles. On a purely mathematical note, it has been pointed out by several authors that the relation between F and a is not one-to-one due to a lack of uniqueness in a. A detailed discussion of this can be found elsewhere. [30]

At high energies, we can make the (semi-classical) correspondence between the orbital angular momentum and impact parameter, $2\ell + 1 \simeq 2K_0 b$, and, in this limit,

$$a(K_0, b) \simeq \mathcal{S}_\ell - 1 \; . \tag{85}$$

This association amounts to making the small wavelength approximation discussed earlier and the scattering amplitude becomes

$$f(\theta) = -iK_0 \int_0^{\infty} b\, db\, J_0(qb) \; [\mathcal{S}(b) - 1] \; . \tag{86}$$

Now $\mathcal{S}(b) = \exp[i\mathcal{X}(b)]$ is the continuation of $\mathcal{S}_\ell$ to real non-integer angular momenta and coincides with the physical S-matrix whenever $K_0 b - 1/2$ has integer value. $\mathcal{S}(b)$ will be referred to as the exact continued (EC) S-matrix. It is important that Eq.(86) does not require, and has not made, the eikonal approximation to the scattering phase shift. The EC phase approach can be viewed as replacing the eikonal phase $\mathcal{X}_0(b)$ in $\mathcal{S}_0(b) = \exp[i\mathcal{X}_0(b)]$ by an improved description using the physical phase shifts, since

$$\mathcal{X}(b) \equiv 2\delta_\ell \ , \qquad 2\ell + 1 = K_0 b \ . \tag{87}$$

The scattering amplitude of Eq.(86) goes beyond the eikonal approximation of Eq.(79). We have adopted the notation of a lower case f for this amplitude to distinguish it from the exact amplitude F.

The formalism generalises to include the Coulomb interaction where the exact partial wave amplitude is now

$$\bar{F}(\theta) = f_C^{pt}(\theta) + \frac{1}{2ik}\sum_{\ell=0}^{\infty}(2\ell+1)\,P_\ell(\cos\theta)\,e^{2i\sigma_\ell}\,[\bar{S}_\ell - 1] \tag{88}$$

where σ_ℓ is the Coulomb phase shift. The $\bar{S}_\ell$ here, obtained by matching to Coulomb functions the solution of the radial Schrödinger equation in the presence of both nuclear and Coulomb interactions, characterise only the deviations from point Coulomb scattering. The EC equivalent of $\bar{S}_\ell$, $\bar{\mathcal{S}}(b)$, is then used in place of the Coulomb modified eikonal S-matrix, $\bar{\mathcal{S}}_0(b)$, in Eq.(80).

A. The Fourier-Bessel expansion

These connections between the partial wave sum and the impact parameter integral representations of the scattering amplitude have also been discussed by Glauber and Franco [31] and Wallace [32]. They showed that a formal connection between F and f can be made using an expansion of the Fourier-Bessel representation, Eq.(84), appropriate to high energies. They clarify that, in writing Eq.(79), in addition to the discrete to continuous variable transformation, only the leading term in the small angle expansion of the Legendre function has been retained. This is the origin of the zeroth order Bessel function $J_0(qb)$. In the complete formal derivation of Wallace [32] an additional operator $W(b)$ multiplies $\mathcal{S}(b)$ such that

$$a(K_0, b) = W(b)\mathcal{S}(b) - 1 \ . \tag{89}$$

It is well documented that the eikonal model works rather well down to lower energies and to larger angles than might be expected. One reason for this is that there is considerable cancellation between the higher order correction terms in the expansion of W about unity, arising from the discrete to continuous variable transformation on the one hand and the small angle approximation on the other. Setting $W(b) = 1$ is therefore a remarkably good approximation.

B. Corrections to the eikonal phase shift

Wallace used the correspondence between the eikonal phase and the expansion of the WKB phase shift as a means of improving the eikonal amplitude. The WKB phase is expressible [32] as an expansion in powers of a parameter $\epsilon = 1/\hbar K_0 v$,

$$\mathcal{X}^{WKB}(b) = \sum_{n=0}^{\infty} \frac{\epsilon^n}{(n+1)!} \mathcal{X}_n(b) \quad , \tag{90}$$

$$\mathcal{X}_n(b) = -\frac{1}{\hbar v} \int_{-\infty}^{\infty} dz \left(\frac{1}{R} \frac{d}{dR} \right)^n [R^{2n} V_{pt}^{n+1}(R)] \quad , \tag{91}$$

with the eikonal phase shift as its $n = 0$ term. The $\mathcal{X}^{WKB}$ are themselves not exact and additional corrections arise [32]. These corrections are also expressible as an expansion in powers of ϵ. Replacing the eikonal phase shift $\mathcal{X}_0$ of Eq.(78) by these expansions leads to an improved phase function.

When the Coulomb interaction is included screening need only be applied in the lowest order (eikonal) term. In higher order terms, V_C appears in quadratic or higher powers of $(V_N + V_C)$. These terms make only finite range modifications to the integrals over z.

The effects of corrections up to third order have been studied and are important for the scattering of nucleons [33]. The effects become more important as the scattering energy is reduced, however, the expansion itself becomes unstable at energies below 25 MeV. For heavier projectiles K_0 is larger and these higher order terms are less important.

X. EIKONAL FEW-BODY MODELS

The extension of the eikonal approximation to few-body problems, the Glauber multiple scattering diffraction theory [29], was proposed to treat high energy hadron-nucleus collisions. In addition to the eikonal assumption, Glauber's model requires that the internal motion of the constituents is slow relative to their centre of mass motion, the adiabatic approximation discussed in Section V.

A. Glauber's few-body model

Here, we are interested in the inverse kinematics picture to the one discussed originally by Glauber in that the projectile is the composite system. The derivation of the cm scattering amplitude is, however, the same in both cases. Our starting point is the adiabatic few-body Schrödinger equation, Eq.(28). We next make an eikonal factorisation of the adiabatic wave function of Eq.(29) of the form

$$\Psi_{\vec{K}_0}^{eik}(\{\vec{r}_i\}, \vec{R}\,) = e^{i\vec{K}_0 \cdot \vec{R}} \omega(\{\vec{r}_i\}, \vec{R}\,)\, \phi_0^{(n)}(\{\vec{r}_i\}). \tag{92}$$

Substituting this wave function into Eq.(28) and following the same arguments as in the point particle case of Section VIII, a first order differential equation for ω is obtained

$$\frac{\partial \omega}{\partial z} = -\frac{i\mu_p}{\hbar^2 K_0} U(\{\vec{R}_j\})\, \omega(\{\vec{r}_i\}, \vec{R}\,) \ . \tag{93}$$

Hence,

$$\begin{aligned} \omega(\{\vec{r}_i\}, \vec{R}\,) &= \exp\left\{-\frac{i}{\hbar v}\int_{-\infty}^{z} U(\{\vec{R}'_j\})dz'\right\} \\ &= \exp\left\{-\frac{i}{\hbar v}\sum_{j=1}^{n}\int_{-\infty}^{z_j} V_{jt}\left(\sqrt{b_j^2 + z_j'^{\,2}}\right) dz'_j\right\}, \end{aligned} \tag{94}$$

where b_j is the impact parameter for constituent j, Figure 4.

The few-body Glauber (FBG) scattering amplitude, for a collision that takes the projectile from an initial state $\phi_0^{(n)}$ to a final state $\phi_\alpha^{(n)}$, can be derived following the same steps as in the point particle case. The post form transition amplitude is now

$$T(\vec{K}_\alpha) = \langle \phi_\alpha^{(n)}\, e^{i\vec{K}_\alpha\cdot\vec{R}} | U(\{\vec{R}_j\}) | \Psi_{\vec{K}_0}^{eik} \rangle, \tag{95}$$

and, in keeping with the adiabatic approximation, if $|\vec{K}_\alpha| = |\vec{K}_0|$, the FBG scattering amplitude is

$$f_0^{(n)}(\vec{K}_\alpha) = -\frac{iK_0}{2\pi}\int d\vec{b}\, e^{i\vec{q}\cdot\vec{b}} \int_{-\infty}^{\infty} dz\ \langle \phi_\alpha^{(n)}|\ U\omega\ |\phi_0^{(n)}\rangle. \tag{96}$$

Using Eq.(93), we obtain

$$f_0^{(n)}(\vec{K}_\alpha) = -\frac{iK_0}{2\pi}\int d\vec{b}\, e^{i\vec{q}\cdot\vec{b}}\, \langle \phi_\alpha^{(n)} | \mathcal{S}_0^{(n)}(\{\vec{b}_j\}) - 1 | \phi_0^{(n)}\rangle, \tag{97}$$

where

$$\mathcal{S}_0^{(n)}(\{\vec{b}_j\}) = \exp\left[i\sum_{j=1}^{n}\mathcal{X}_{0j}(b_j)\right] = \prod_{j=1}^{n}\mathcal{S}_{0j}(b_j). \tag{98}$$

Thus the total phase shift is the sum of the phase shifts for the scattering of each of the projectile's constituents. This property of phase shift additivity is a direct consequence of the linear dependence of eikonal phases on interaction potentials.

A crucial point to make here is that this few-body model applies only when the momentum transfer between the projectile and target is small relative to the incident centre of mass momentum, since we have continued to assume that $\vec{q}\cdot\vec{R} \approx \vec{q}\cdot\vec{b}$. This is certainly a good approximation for elastic and mildly inelastic collisions.

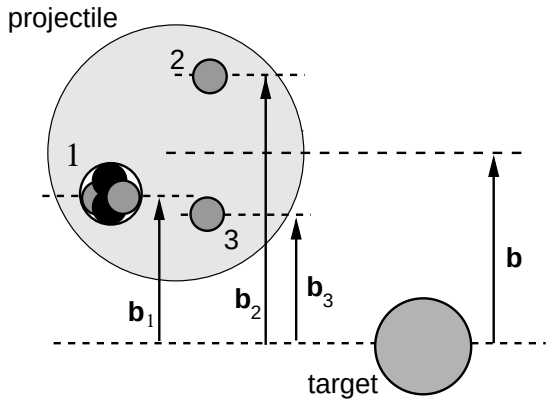

FIG.4 The full projectile S-matrix is obtained from the individual S-matrices of its constituent clusters, each evaluated at its own impact parameter.

B. Multiple scattering interpretation

The few-body Glauber model can be interpreted as a multiple scattering series by defining the profile functions Γ_j, which are proportional to the transition amplitudes for $j+t$ scattering,

$$\Gamma_j(\vec{b}_j) = 1 - \mathcal{S}_{0j}(\vec{b}_j) \ . \tag{99}$$

Thus

$$\begin{aligned} \mathcal{S}_0^{(n)}(\{\vec{b}_j\}) &= \prod_{j=1}^{n} (1-\Gamma_j) \\ &= 1 - \sum_j \Gamma_j + \sum_{j\neq k} \Gamma_j\Gamma_k + \cdots (-)^n \prod_j \Gamma_j \ . \end{aligned} \tag{100}$$

Substituted into Eq.(97) for the FBG amplitude we see that the terms linear in Γ_j account for the single scattering (impulse approximation) contributions to the amplitude due each of the constituents in the projectile. Subsequent terms provide double, triple, etc. scattering corrections. Note that the order of the multiple scattering can be at most n since, due to the forward (small angle) scattering assumption of the eikonal model, once the target and a particular constituent of the projectile have interacted, they will not meet again. This would involve back scattering.

C. Coulomb interactions

When one or more of the clusters is charged we follow the same Coulomb screening arguments used above. Now, for each charged cluster j, $\mathcal{X}_{0C}^j(b_j) = \mathcal{X}_{0\rho}^j(b_j) + \mathcal{X}_a^j$. Since the screening phases $\mathcal{X}_a^j = -2\eta_j \ln(2K_0 a)$ depend linearly on the Sommerfeld parameter of each cluster η_j

and $\eta = \sum_j \eta_j$, these phases add to give the screening phase appropriate to the projectile $\mathcal{X}_a$. The few-body eikonal amplitude in the presence of nuclear and Coulomb forces, analogous to $\bar{f}_0$ of Eq.(80), is therefore (omitting the overall screening phase)

$$\bar{f}_0^{(n)}(\theta) = f_{pt}(\theta) - iK_0\int_0^\infty b\,db\; J_0(qb)\; e^{i\mathcal{X}_{pt}}\langle\phi_0^{(n)}|\bar{\mathcal{S}}_0^{(n)} - 1|\phi_0^{(n)}\rangle, \tag{101}$$

where

$$\bar{\mathcal{S}}_0^{(n)}(\{\vec{b}_j\}) = \exp\left\{i\sum_{j=1}^{n}[\mathcal{X}_{0N}^j(b_j) + \mathcal{X}_{0\rho}^j(b_j)] - i\mathcal{X}_{pt}(b)\right\}. \tag{102}$$

D. The recoil limit solution revisited

The few-body Glauber approach provides further insight into the recoil limit solution discussed in Section VII. It was shown there that in the limit when just one of the projectile clusters c interacts with the target, the few-body adiabatic scattering amplitude can be factorized into an amplitude describing the scattering of a point-like particle with the mass of the projectile, interacting via V_{ct}, and the appropriate form factor $F_{\alpha 0}$ that describes the projectile's internal structure. In the Glauber framework, the eikonal phase shifts depend only on the incident velocities of the clusters, which are of course the same as that of the whole projectile. Hence, the S-matrices for the clusters are independent of their mass, and the point-like amplitude in the recoil limit approximation is the amplitude for the independent scattering of cluster c, evaluated at a different momentum transfer. In fact, the cm momentum of the projectile enters the amplitude expression in two places: as a multiplying factor outside the b integral and in the argument of the Bessel function. Thus the cross section in the recoil limit, defined in Eq.(60), is, in the Glauber framework

$$\left(\frac{d\sigma(q)}{d\Omega}\right)_\alpha = |F_{\alpha 0}(\gamma_c\vec{q})|^2\;\beta_c^2\;\left(\frac{d\sigma(\beta_c q)}{d\Omega}\right)_c, \tag{103}$$

where the point cross section of Eq.(60) has been replaced by the physical cross section for the scattering of cluster c, evaluated at a different momentum transfer. The factor, β_c, is

$$\beta_c = \frac{K_0}{K_c} = \frac{m_p}{m_c}\left(\frac{m_c + m_t}{m_p + m_t}\right), \tag{104}$$

where K_c is the cm momentum of cluster c.

Eq.(103) is useful if the differential cross sections for both c+t and p+t scattering at the same laboratory energy are known, since it can give information about the structure of the projectile through the form factor $F_{\alpha 0}$, provided of course that the recoil approximation is valid. Examples of such systems, as discussed in Section VII, are single neutron halo nuclei, such as ^{19}C, which can be treated as a two-cluster (^{18}C+n) system in which the ^{18}C+target interaction should dominate the ^{19}C scattering process.

E. Non-eikonal corrections

The additivity of phases property of the Glauber approach suggests that improvements can be made by replacing each eikonal phase shift function with a more accurate one. Such non-eikonal modifications to the phase shifts of each cluster can be introduced as was discussed for the case of point scattering earlier. Indeed, recent studies have shown that including corrections up to third order in ϵ_j ($\propto K_j^{-2}$, where K_j is the cluster-target cm wave number) improves the accuracy of the few-body calculations to lower energies and larger scattering angles. For the scattering of two- and three-body projectiles, such as the deuteron and the halo nuclei, ^{11}Be and ^{11}Li, comparisons have been made with the more accurate adiabatic model calculations.

However, rather than develop and sum the expansion for the phase shifts in powers of ϵ, a much more efficient approach is to solve directly the radial Schrödinger equation for each cluster-target two-body system at the required impact parameters and hence non-integer orbital angular momenta $\lambda_j = b_j K_j - 1/2$. No eikonal assumptions need therefore be made, however the model would still retain the adiabatic and additivity of phases approximations. This is done by replacing each eikonal phase shift $\mathcal{S}_{0j}(b)$ by its EC equivalent, $\mathcal{S}_j(b)$, defined in Section IX.

To generalise the formalism to include the Coulomb interaction, the EC equivalent, $\bar{\mathcal{S}}_j(b_j)$, of the charged cluster S-matrix, in the presence of both Coulomb and nuclear interactions, replaces the corresponding eikonal one $\bar{\mathcal{S}}_{0j}(b_j)$.

A subtlety of this approach is that, since each charged cluster S-matrix contains deviations from point Coulomb scattering at its own impact parameter, b_j, the point Coulomb phase shift must be incorporated within the cm b integral. Thus

$$\bar{\mathcal{S}}^{(n)} = \prod_{j=1}^{n} \bar{\mathcal{S}}_j(b_j) \, \exp\left[\sum_{k=1}^{n} i\mathcal{X}_{pt}^{k}(b_k) - i\mathcal{X}_{pt}(b)\right]. \tag{105}$$

XI. REACTION OBSERVABLES

Few-body impact parameter methods provide a convenient framework for calculating probabilities and cross sections for a variety of processes involving peripheral collisions between composite projectiles and stable targets. As has been emphasised throughout these notes, projectiles composed of a few loosely-bound clusters require non-perturbative methods due to the importance of higher order intermediate state couplings. Impact parameter methods in general have a long history of being applied to reactions of loosely-bound nuclei that predates the work of Glauber. In particular, stripping processes, such as in deuteron-induced reactions, have been studied using approaches developed by Serber [34]. Variants of such methods are still in use today due to the simple geometric properties of the reaction processes at high energies.

In the few-body Glauber model, the differential cross section for the scattering process

defined by Eq.(97) is

$$\left(\frac{d\sigma}{d\Omega}\right)_\alpha = |f^{(n)}(\vec{K}_\alpha)|^2, \tag{106}$$

and the total cross section for populating the final state α is thus

$$\begin{aligned}\sigma_\alpha &= \int d\Omega\ |f^{(n)}(\vec{K}_\alpha)|^2 \\ &= \int d\vec{b}\ |\langle\phi_\alpha^{(n)}|\mathcal{S}^{(n)}|\phi_0^{(n)}\rangle - \delta_{\alpha 0}|^2\ .\end{aligned} \tag{107}$$

It should again be noted however that such an expression is only valid at high beam energies and low excitation energies since energy conservation is not respected in this model. When $\alpha = 0$, the total elastic cross section is

$$\sigma_{el} = \int d\vec{b}\ |1 - \langle\phi_0^{(n)}|\mathcal{S}^{(n)}|\phi_0^{(n)}\rangle|^2. \tag{108}$$

The total cross section is also obtained from the elastic scattering amplitude, employing the optical theorem, to give

$$\sigma_{tot} = 2\int d\vec{b}\left[1 - \mathcal{R}e\ \langle\phi_0^{(n)}|\mathcal{S}^{(n)}|\phi_0^{(n)}\rangle\right]. \tag{109}$$

Hence, the total reaction cross section, defined as the difference between these total and elastic cross sections, is

$$\sigma_R = \int d\vec{b}\left[1 - |\langle\phi_0^{(n)}|\mathcal{S}^{(n)}|\phi_0^{(n)}\rangle|^2\right]. \tag{110}$$

For projectiles with just one bound state, any excitation due to interaction with the target will be into the continuum. For such nuclei, which include the deuteron and many of the neutron halo nuclei (such as ^{6}He and ^{11}Li), it is possible to describe elastic breakup channels in which the target as well as each cluster in the projectile remain in their ground states. For simplicity of notation, we assume a two-body projectile with continuum wave function $\phi_{\vec{k}}$, where $\vec{k}$ is the relative momentum between the two clusters, and $\mathcal{S} = \mathcal{S}^{(2)}(b_1, b_2) = \mathcal{S}_1(b_1)\mathcal{S}_2(b_2)$ is understood. Elastic breakup, also referred to as diffractive dissociation, has amplitudes

$$f(\vec{k},\theta) = -iK_0\int d\vec{b}\, e^{i\vec{q}\cdot\vec{b}}\,\langle\phi_{\vec{k}}|\mathcal{S}|\phi_0\rangle. \tag{111}$$

Making use of the completeness relation (when there is only one bound state)

$$\int d\vec{k}\ |\phi_{\vec{k}}\rangle\langle\phi_{\vec{k}}| = 1 - |\phi_0\rangle\langle\phi_0| \tag{112}$$

the total elastic breakup cross section is

$$\sigma_{bu} = \int d\vec{b}\left[\langle\phi_0|\ |\mathcal{S}|^2|\phi_0\rangle - |\langle\phi_0|\mathcal{S}|\phi_0\rangle|^2\right]\ . \tag{113}$$

The difference between the reaction and elastic breakup cross section is the absorption cross section,

$$\sigma_{abs} = \int d\vec{b} \left[1 - \langle \phi_0 |\ |\mathcal{S}|^2 | \phi_0 \rangle \right] \ , \tag{114}$$

which represents the cross section for excitation of either the target or one or both of the projectile clusters.

The above formula can be understood by examining the physical meaning of $|\mathcal{S}|^2$ ($= |\mathcal{S}_1|^2 |\mathcal{S}_2|^2$). The square modulus of each cluster S-matrix element, $|\mathcal{S}_j|^2$ represents the probability that it survives intact following interaction with the target at impact parameter $\vec{b}_j$. That is, at most, it is elastically scattered. At large impact parameters $|\mathcal{S}_j|^2 \to 1$ since the constituent passes too far from the target. The quantity $1 - |\mathcal{S}_j|^2$ is therefore the probability that cluster j interacts with the target and is absorbed from the system. Such a simple picture is useful when studying stripping reactions in which one or more of the projectile's clusters are removed by the target while the rest of the projectile survives. Thus, the cross section for stripping cluster 1 from the projectile, with cluster 2 surviving, is given by

$$\sigma_{str} = \int d\vec{b}\ \langle \phi_0 | |\mathcal{S}_2|^2 [1 - |\mathcal{S}_1|^2] | \phi_0 \rangle. \tag{115}$$

This cross section is seen to vanish if the interaction V_{1t} of constituent 1 with the target is non-absorptive, and hence $|\mathcal{S}_1| = 1$.

XII. HIGH ENERGY EIKONAL LIMIT

This Section demonstrates, using the high energy limit and a simple two-body structure model, that the few-body structure of a nucleus has significant implications for the calculation and interpretation of cross sections. These are important considerations when measured cross sections are used to deduce nuclear properties, such as their root mean squared (rms) matter radii.

Theoretically, the situation is simpler at high energy because the interaction between each projectile constituent and the target becomes essentially absorptive. The constituent-target S-matrix elements $\mathcal{S}_{0j}(b_j)$ can also be calculated reliably using the optical limit of Glauber theory [35] in which correlations, internal to each j and to t, are neglected. The $\mathcal{S}_{0j}$ are then calculated, in eikonal approximation, from the first-order multiple scattering ($t\rho\rho$) approximation to V_{jt} using the one-body densities ρ_j and ρ_t of j and the target and an effective nucleon-nucleon (NN) amplitude f_{NN}. For a single nucleon, then $\rho_j(x) = \delta(\vec{x})$.

Explicitly, the $\mathcal{S}_{0j}$ in the optical limit (OL) are

$$\mathcal{S}_{0j}^{OL}(b) = e^{i\chi_{0j}(b)} = \exp\left[i \int_{-\infty}^{\infty} dz\, \mathcal{O}_{jt}(R) \right], \tag{116}$$

where $\mathcal{O}_{jt}$ is the double-folding integral

$$\mathcal{O}_{jt}(R) = \int d\vec{x}_j \int d\vec{x}_t\, \rho_j(x_j)\, \rho_t(x_t)\, f_{NN}(r_{jt}), \tag{117}$$

with $r_{jt} = |\vec{R} + \vec{x}_j - \vec{x}_t|$. Assuming a purely absorptive and zero-range NN amplitude then it is usual [35] to associate

$$f_{NN}(\vec{r}) = \frac{i\sigma_{NN}}{2}\,\delta(\vec{r}) \ , \tag{118}$$

where σ_{NN} is the isospin average of the free NN total cross sections. This is sometimes modified to account (partially) for the effects of scattering in the nuclear medium.

While, in the $\mathcal{S}_{0j}^{OL}$, we have neglected correlations internal to each constituent and the target, we can choose to retain or neglect the few-body correlations between the constituents j of the projectile. Retaining these, the projectile few-body elastic S-matrix, constructed from the $\mathcal{S}_{0j}^{OL}$, Eq.(98), is

$$\mathcal{S}_p^{FB}(b) = \langle\phi_0^{(n)}|\prod_j \mathcal{S}_{0j}^{OL}(b_j)|\phi_0^{(n)}\rangle. \tag{119}$$

If, on the other hand, we also neglect these few-body correlations then the projectile optical limit S-matrix, $\mathcal{S}_p^{OL}(b)$ must be calculated from Eq.(116), where the overlap $\mathcal{O}_{pt}$ is calculated from the projectile one-body density ρ_p according to Eq.(117). This is equivalent [36] to retaining only the first term in the cumulant expansion of the projectile phase shift function $\mathcal{X}_0(\{b_j\}) = \sum_j \mathcal{X}_{0j}(b_j)$.

It is also instructive to note that, when each $\mathcal{S}_{0j}$ is described using the optical limit, Eq.(116), then the projectile OL S-matrix, $\mathcal{S}_p^{OL}$, is equivalent to approximating Eq.(119) by its no-breakup or folding model potential eikonal S-matrix, Eq.(4), i.e.

$$\mathcal{S}_p^{OL}(b) = \exp\left[i\langle\phi_0^{(n)}|\mathcal{X}_0(\{b_j\})|\phi_0^{(n)}\rangle\right] = \exp[i\mathcal{X}_p(b)]. \tag{120}$$

This is to be contrasted with the correlated few-body expression,

$$\mathcal{S}_p^{FB}(b) = \langle\phi_0^{(n)}|\exp[i\mathcal{X}_0(\{b_j\})]|\phi_0^{(n)}\rangle. \tag{121}$$

The effects of an explicit treatment of projectile breakup channels can therefore be examined using Eqs.(121) and (120). These equations clarify that the assumption of uncorrelated particle motions, which underlies the optical limit of the eikonal theory, is inconsistent with a realistic treatment of the continuum excitations of weakly bound few-body nuclei.

To evaluate $\mathcal{S}_p^{FB}$ and $\mathcal{S}_p^{OL}$ using realistic theoretical inputs is a reasonably involved numerical task. We therefore use a simple two-body model, involving Gaussian densities, to expose the consequences of the two calculations. For this analysis the zero range t_{NN} is adequate to clarify these differences.

A. Binary cluster model

We consider a two-body projectile with mass m_p, consisting of valence and core clusters of masses m_v and m_c bound in a state of relative motion, Figure 5. For simplicity the internal densities of the clusters are described by single Gaussian functions with ranges α_c and α_v, i.e.

$$\rho_c(r) = m_c g^{(3)}(\alpha_c, r) \ \ , \tag{122}$$

and similarly for ρ_v. Here $g^{(3)}$ is the normalised three-dimensional Gaussian function

$$g^{(3)}(\gamma, r) = (\sqrt{\pi}\gamma)^{-3} \exp(-r^2/\gamma^2), \tag{123}$$

which has mean squared radius $\langle r^2 \rangle = 3\gamma^2/2$. If we also assume that the relative motion wavefunction $\phi_0^{(2)}(\vec{r})$ of the two clusters is a $0s$ oscillator state of range parameter α then of course

$$|\phi_0^{(2)}(\vec{r})|^2 = g^{(3)}(\alpha, r) \quad , \tag{124}$$

with mean squared c-v separation $\langle r^2 \rangle = 3\alpha^2/2$.

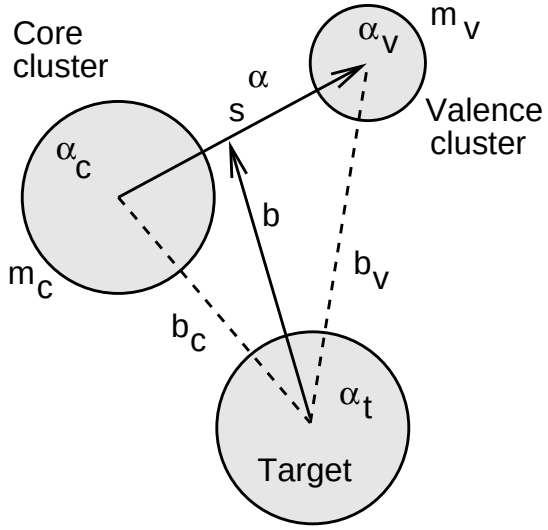

FIG.5 The two-cluster projectile coordinates relative to the target . The co-ordinate z-axis, the projectile beam direction, is directed into the page.

This model allows us to construct explicitly the projectile single-particle density needed for the OL calculation. Convoluting the intrinsic cluster densities with their motions about the cm of the projectile, this is

$$\rho_p(r) = m_c g^{(3)}(\hat{\alpha}_c, r) + m_v g^{(3)}(\hat{\alpha}_v, r) \tag{125}$$

where the new Gaussian range parameters are

$$\hat{\alpha}_v^2 = \alpha_v^2 + \left(\frac{m_c \alpha}{m_p}\right)^2 \quad , \quad \hat{\alpha}_c^2 = \alpha_c^2 + \left(\frac{m_v \alpha}{m_p}\right)^2 \quad . \tag{126}$$

The model thus produces a two component projectile density, due to v and c, containing different numbers of nucleons, and with different spatial extensions. Such simple two component forms have been used widely to model density distributions of light exotic nuclei [24]. The mean squared radius of p, $\langle r^2 \rangle_p$, satisfies

$$\begin{aligned} m_p \langle r^2 \rangle_p &= m_c \langle r^2 \rangle_c + m_v \langle r^2 \rangle_v + (m_v m_c/m_p) \langle r^2 \rangle \\ &= (3/2) \left(m_v \hat{\alpha}_v^2 + m_c \hat{\alpha}_c^2 \right) \quad . \end{aligned} \tag{127}$$

The model shows that fixing $\rho_p(r)$, by a given (m_c,m_v) mass split and choice of the two convoluted ranges ($\hat{\alpha}_c$,$\hat{\alpha}_v$), does not specify the underlying structure of the projectile. Eq.(126) shows that any fixed density is consistent with an infinite number of two cluster structures having different c and v rms sizes and separations. Specifically, for a fixed projectile density, α can take on all values from zero to an upper limit

$$\alpha_{max} = \min\left[(m_p/m_c)\hat{\alpha}_v, (m_p/m_v)\hat{\alpha}_c\right] \quad , \tag{128}$$

at which one or other of the cluster densities must be pointlike. If one of the original clusters is pointlike, e.g. $\alpha_v = 0$, then fixing $\hat{\alpha}_v$ and $\hat{\alpha}_c$ does uniquely determine α and hence α_c.

Assuming the target nucleus is also described by a Gaussian density of range α_t, then the OL and FB expressions for $\mathcal{S}_p$ take particularly simple forms. Now, in Eq.(120),

$$\mathcal{X}_p(b) = i\frac{\sigma_{NN}}{2} m_t[m_c g^{(2)}(\hat{\alpha}_{ct}, b) + m_v g^{(2)}(\hat{\alpha}_{vt}, b)], \tag{129}$$

where $g^{(2)}(\gamma, b) = (\sqrt{\pi}\gamma)^{-2}\exp(-b^2/\gamma^2)$ is the normalised two-dimensional Gaussian, $\hat{\alpha}_{vt}^2 = \hat{\alpha}_v^2 + \alpha_t^2$, and similarly for $\hat{\alpha}_{ct}^2$. The FB S-matrix, Eq.(121), is

$$\mathcal{S}_p^{FB}(b) \;=\; \int d\vec{s}\, g^{(2)}(\alpha, s)\exp[i\mathcal{X}_{0c}(b_c) + i\mathcal{X}_{0v}(b_v)], \tag{130}$$

$$\mathcal{X}_{0j}(b_j) \;=\; i\frac{\sigma_{NN}}{2} m_t m_j g^{(2)}(\alpha_{jt}, b_j) \tag{131}$$

with $\vec{s}$ the projection of $\vec{r}$ in the impact parameter plane and $b_c = |\vec{b} - m_v\vec{s}/m_p|$ and $b_v = |\vec{b} + m_c\vec{s}/m_p|$ are the impact parameters of the core and valence clusters, Figure 5. In this case $\alpha_{jt}^2 = \alpha_j^2 + \alpha_t^2$, from the convolution of the each cluster and the target density. The two expressions are seen to agree only in the $\alpha \to 0$ limit, when the two-body model reverts to a description based on a single centre, and so the two-body correlations are removed.

B. Reaction cross sections

The OL and FB approaches have implications for the calculated elastic scattering differential cross section and the total and integrated elastic cross sections, Eqs.(109) and (108) of Section XI. To demonstrate these effects, Figure 6 shows the calculated reaction cross sections, Eq.(110),

$$\sigma_R = 2\pi\int_0^\infty db\, b\left[1 - |\mathcal{S}_p(b)|^2\right] \quad , \tag{132}$$

using σ_{NN}=4.11 fm^2, appropriate to 800 MeV per nucleon projectile incident energy. We take as a representative case m_p=10, $\langle r^2\rangle_p^{1/2}$=3.10 fm, with ($m_c$,$m_v$)=(8,2) and m_t=12, $\langle r^2\rangle_t^{1/2}$=2.32 fm. The range parameters $\hat{\alpha}_v$ and $\hat{\alpha}_c$ are such that $m_v\hat{\alpha}_v^2 = m_c\hat{\alpha}_c^2$, so the c and v make equal contributions to the projectile rms matter radius, Eq. (127), ensuring sufficient emphasis is given to the valence particles.

These parameters fix $\rho_p(r)$, $\mathcal{S}_p^{OL}$, and hence the OL reaction cross section, the dashed line in Figure 6, independently of the underlying cluster sizes and separations. The FB cross

sections are shown by the solid symbols and line in the figure as a function of the rms separation of c and v. As the figure indicates, the c and v internal densities have to become more localised at large rms separations to maintain the fixed ρ_p. The limiting situation is where one valence cluster is pointlike when the maximum differences between the cross sections calculated using the FB and OL theories are manifest.

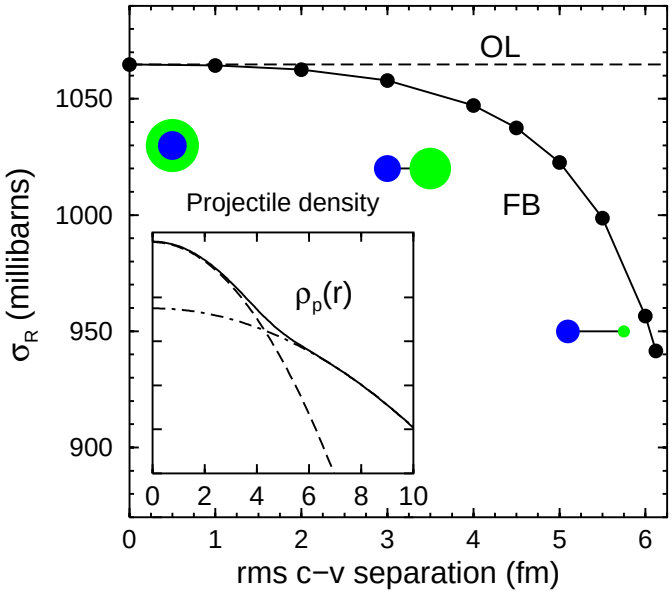

FIG.6 Few-body (FB) and optical limit (OL) calculations of reaction cross sections for a m_p=10 projectile, composed of m_c=8 and m_v=2 clusters, as a function of the assumed rms separation of c and v. All calculations correspond to the same projectile one-body density, shown as an inset.

C. The role of breakup

Although the calculations of Figure 6 use a simple model, the key result, that the FB reaction cross section is smaller than that of the OL calculation, is a quite general consequence of Eqs.(120) and (121) when the underlying constituent-target interactions are entirely absorptive, and hence the $\mathcal{X}_{0j}$ are purely imaginary. This follows from the real variable inequality [37]

$$\exp(y) \geq 1 + y, \tag{133}$$

which results from the upward concavity of the exponential function. From this follows the similar inequality between expectation values of an Hermitian operator Y, i.e.

$$\langle \exp(Y) \rangle \geq \langle 1 + Y \rangle, \tag{134}$$

and, writing $Y = F - \langle F \rangle$, where F is clearly also Hermitian, the latter inequality can be recast as

$$\langle \exp(F) \rangle \geq \exp\langle F \rangle. \tag{135}$$

Therefore with $F = i\mathcal{X}_0(\{b_j\})$, which is real for absorptive V_{jt}, and taking the projectile ground state expectation value, proves that for all b, $\mathcal{S}_p^{FB}(b) \geq \mathcal{S}_p^{OL}(b)$, where $|\mathcal{S}_p(b)| \leq 1$. It follows that $\sigma_R^{OL} \geq \sigma_R^{FB}$.

It should be pointed out, therefore, that including the effects of breakup of the few-body projectile, through Eq.(121), actually reduces the calculated reaction cross sections when compared to the use of the no-breakup optical limit, using Eq.(120). As is revealed by the inequality $\mathcal{S}_p^{FB} \geq \mathcal{S}_p^{OL}$, overall, the explicit treatment of the few-body nature of the projectile results in the collision being more transparent and less absorptive. The reason for this is that, in many configurations of the spatially separated constituents, they do not overlap and interact with the target. This additional transparency, due to the granular nature of the projectile, is shown here to more than compensate for the additional absorption due to removal of flux from the elastic channel into the, now included, breakup channels.

It follows that if one compares measured high energy cross sections with those obtained from σ_R^{OL}, to deduce interaction radii, or nuclear sizes, then these sizes will be an underestimate of the actual spatial extent of the nuclei in those cases where the projectile has a well developed few-body internal structure.

Acknowledgments

This work was supported by the United Kingdom EPSRC through grant GR/J95867.

---

[1] Austern N (1970) *Direct Nuclear Reaction Theories*. New York: Wiley.
[2] Satchler G R (1983) *Direct Nuclear Reactions*. Oxford: Clarendon Press.
[3] Alder K and Winther A (1975) *Electromagnetic Excitation*. Amsterdam: North Holland
[4] Baur G and Rebel H (1994) Coulomb dissociation studies as a tool of nuclear astrophysics. *Journal of Physics G* **20**: 1.
[5] Esbensen H (1999) Reactions of halo states: Coulomb excitation. In Broglia R A and Hansen P G (eds) *International School of Heavy ion physics*, 4th course: Exotic nuclei, pp71-92. Singapore: World Scientific Press.
[6] Melezhik V S and Baye D (1999) Non-perturbative time-dependent approach to breakup of halo nuclei. *Physical Review* **59**: 3232; and references therein.
[7] Kamimura M, Yahiro M, Iseri Y, Sakuragi Y, Kameyama H and Kawai M (1986) Coupled-channels theory of breakup processes in nuclear reactions. *Progress in Theoretical Physics Supplement* **89**: 1.
[8] Austern N, Iseri Y, Kamimura M, Kawai M, Rawitscher G and Yahiro M (1987) Continuum discretized coupled-channels calculations for three-body models of deuteron-nucleus reactions. *Physics Reports* **154**:125.
[9] Watanabe S (1958) High energy scattering of the deuteron by complex nuclei. *Nuclear Physics* **8**: 484.
[10] Sakuragi Y, Yahiro M and Kamimura M (1986) Microscopic coupled-channels study of scattering and breakup of light heavy-ions. *Progress in Theoretical Physics Supplement* **89**: 136.

[11] Thompson I J (1988) Coupled reaction channels calculations in nuclear physics. *Computer Physics Reports* **7**: 167; Thompson I J (2000) FRESCO users' manual, University of Surrey, UK.
[12] Ohlson G G (1965) Kinematic relations in reactions of the form A+B→C+D+E. *Nuclear Instruments and Methods* **37**: 240.
[13] Johnson R C and Soper P J R (1970) Contribution of deuteron breakup channels to deuteron stripping and elastic scattering. *Physical Review C* **1**: 976.
[14] Christley J A, Al-Khalili J S, Tostevin J A and Johnson R C (1997) Four-body adiabatic model applied to elastic scattering. *Nuclear Physics* **A624**: 275.
[15] Amakawa H, Yamaji S, Mori A and Yazaki K (1979) Adiabatic treatment of elastic deuteron-nucleus scattering. *Physics Letters* **82B**: 13.
[16] Thompson I J and Nagarajan M A (1983) Elastic breakup of 70 MeV ^{7}Li ions on lead. *Physics Letters* **123B**: 379.
[17] Yahiro M, Tostevin J A and Johnson R C (1989) Three-body treatment of the final state in the (^{3}He,pp) reaction on medium mass nuclei. *Physical Review Letters* **62**: 133.
[18] Gönül B and Tostevin J A (1996) Adiabatic treatment of final states in (p,d*) reactions. *Physical Review C* **53**: 2949.
[19] Johnson R C, Stephenson E J and Tostevin J A (1989) Nature of the amplitudes missing from adiabatic distorted wave models of medium energy (d,p) and (p,d) reactions. *Nuclear Physics* **A505**: 26.
[20] Johnson R C and Tandy P C (1974) An approximate three-body theory of deuteron stripping. *Nuclear Physics* **A235**: 56; Laid A, Tostevin J A and Johnson R C (1993) Deuteron breakup effects in transfer reactions using a Weinberg state expansion method. *Physical Review C* **48**: 1307.
[21] Amakawa H, Austern N and Vincent C M (1984) Quasiadiabatic dynamics of deuteron stripping and breakup reactions. *Physical Review C* **29**: 699.
[22] Stephenson E J, Bacher A D, Berg G P A, Cupps V R, Foster C C, Hodiwalla N, Li P, Lisantti J, Low D A, Miller D W, Olmer C, Opper A K, Park B K, Sawafta R, Wissink S W, Tostevin J A, Coley D A and Johnson R C (1990) Enhancement of the near-side component in quasiadiabatic calculations of the ^{66}Zn(d,p)^{67}Zn reaction. *Physical Review C* **42**: 2562.
[23] Johnson R C, Al-Khalili J S and Tostevin J A (1997) Elastic scattering of halo nuclei. *Physical Review Letters* **79**: 2771.
[24] Hansen P G, Jensen A S and Jonson B (1995) Nuclear halos. *Annual Review of Nuclear and Particle Science* **45** 591; Tanihata I (1996) Neutron halo nuclei. *Journal of Physics G* **22**: 157.
[25] Tostevin J A, Rugmai S and Johnson R C (1998) Coulomb dissociation of light nuclei. *Physical Review C* **57**: 3225.
[26] Vincent C M and Fortune T (1970) New method for distorted-wave analysis of stripping to unbound states. *Physical Review C* **2**: 782.
[27] Baur G and Trautmann D (1972) The Coulomb break-up of the deuteron. *Nuclear Physics* **A191**: 321; Nordsieck A (1954) Reduction of an integral in the theory of bremsstrahlung. *Physical Review* **93**: 785.
[28] Banerjee P, Tostevin J A and Thompson I J (1998) Coulomb breakup of ^{11}Be and ^{19}C. *Physical Review C* **58**: 1042; Coulomb breakup of two-neutron halo nuclei. *Physical Review C* **58**: 1337.
[29] Glauber R J (1959) High-energy Collision theory. In Brittin W E (ed) *Lectures in*

Theoretical Physics, Vo1. 1: 315. New York: Interscience.
[30] Newton R G (1966) *Scattering theory of waves and particles*. New York: McGraw-Hill.
[31] Franco V and Glauber R J (1966) High-energy deuteron cross sections. *Physical Review* **142**: 1195.
[32] Wallace S J (1973) High energy expansions of scattering amplitudes. *Physical Review D* **8**: 1846; Wallace S J (1973) Eikonal Expansion. *Annals of Physics* **78**: 190.
[33] Brooke J M, Al-Khalili J S and Tostevin J A (1999) Noneikonal calculations for few-body projectiles. *Physical Review C* **59**: 1560.
[34] Serber R (1947) The production of high energy neutrons by stripping. *Physical Review* **72**: 1008.
[35] Alkhazov G D, Belostotsky S L and Vorobyov A A (1978) Scattering of 1 GeV protons on nuclei. *Physics Reports* **42**: 89.
[36] Franco V and Varma G K (1978) Collisions between composite particles at medium and high energies. *Physical Review C* **18**: 349.
[37] Johnson R C and Goebel C J (2000) Inequality for high energy nuclear reaction cross sections. *Physical Review C* **62**: 027603.